

## SUPPORTING INFORMATION

# Oxime Metathesis: Tunable and Versatile Chemistry for Dynamic Networks

Luca Pettazzoni<sup>a</sup>, Marta Ximenis<sup>b</sup>, Francesca Leonelli<sup>a</sup>, Giulia Vozzolo<sup>b</sup>, Enrico Bodo<sup>a</sup>, Fermin Elizalde<sup>b</sup>, Haritz Sardon<sup>b,c\*</sup>

<sup>a</sup>Department of Chemistry, Sapienza Università di Roma, Piazzale Aldo Moro 5, 00185 Rome, Italy Address here.

<sup>b</sup>POLYMAT University of the Basque Country UPV/EHU, Joxe Mari Korta Center, Avda. Tolosa 72, 20018 Donostia-San Sebastián, Spain

<sup>c</sup>Department of Polymers and Advanced Materials: Physics, Chemistry and Technology, Faculty of Chemistry, University of the Basque Country. UPV/EHU, Donostia-San Sebastián 20018, Spain.

Corresponding author: Haritz Sardon. Email: haritz.sardon@ehu.eus

## TABLE OF CONTENTS

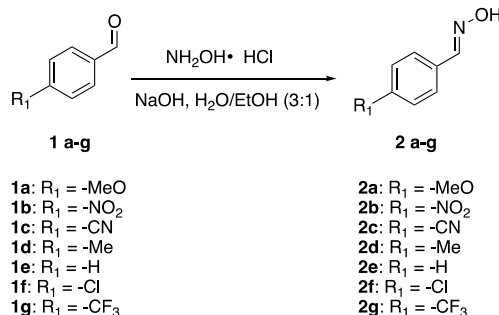
MATERIALS AND METHODS.....	S1
MOLECULAR MODEL REACTIONS.....	S5
COMPUTATIONAL METHODS.....	S5
SUBSTITUENT EFFECT STUDY.....	S7
HYDROLYTIC STABILITY: IMINES VS OXIMES.....	S11
NETWORK CROSSLINKING.....	S12
RHEOLOGICAL CHARACTERIZATION.....	S14
REPROCESSING STUDIES.....	S15
NMR SPECTRA.....	S16
GC-MS CHROMATOGRAM AND MASS SPECTRA.....	S33
REFERENCES.....	S35

## MATERIALS AND METHODS

4-methoxybenzaldehyde (98%), 4-nitrobenzaldehyde (98%), 4-cyanobenzaldehyde (98%), 4-methylbenzaldehyde (98%), benzaldehyde (98%), 4-(trifluoromethyl)benzaldehyde (98%), 4-chlorobenzaldehyde (98%), hydroxylamine hydrochloride (99%), sodium hydroxide (98%, pellets), toluene-4-sulfonic acid monohydrate (99%), methanesulfonic acid (99%), 1, 5, 7-triazabicyclo[4.4.0]dec-5-ene (98%), 1,8-diazabicyclo[5.4.0]undec-7-ene (98%) 1-bromohexane (98%), 4-bromo-1-butene (97%), 3-bromo-1-propene (97%), trimethylolpropane tris(3-mercaptopropionate) (≥95%), 2,2-dimethoxy-2-phenylacetophenone (DMPA) (99%), potassium carbonate (99%), sodium sulfate (99%, anhydrous), silica flash (high-purity grade, pore size 60 Å, 230-400 mesh particle size, 40-63 μm particle size), ethanol, ethyl acetate, hexane and acetone were purchased from Sigma-Aldrich and used without further purification. <sup>1</sup>H-NMR and <sup>13</sup>C-NMR spectra were recorded through a Bruker AVANCE™-400 spectrometer (400.13 MHz, 100.61 MHz). NMR spectra were determined in C<sub>6</sub>D<sub>6</sub> and chemical shifts were expressed in ppm (δ) relative to the residual solvent peak (respectively 7.16 ppm for <sup>1</sup>H-NMR and 128.1 ppm for <sup>13</sup>C-NMR for C<sub>6</sub>D<sub>6</sub>). GC-MS analysis was performed on a Shimadzu QP5000, using Electronic Ionization as the ionization method and Equity™-5 as a chromatographic column. Retention time is given in

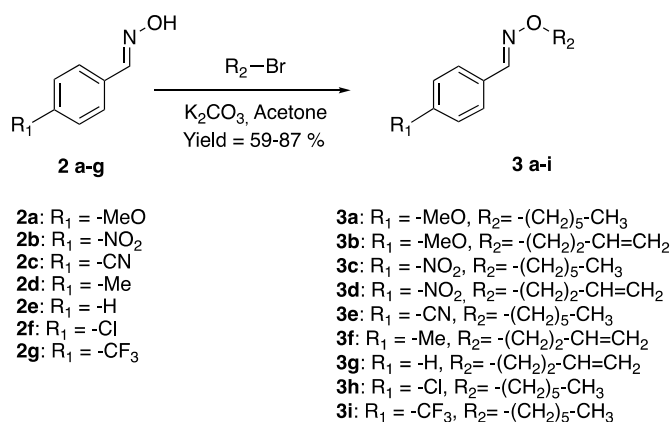
minutes. Fourier transform infrared spectroscopy FTIR spectra were obtained by FTIR spectrophotometer (Nicolet IS20 FTIR, Thermo Scientific Inc., USA) using attenuated total reflectance (ATR) technique (Golden Gate, spectra Tech). Spectra were recorded between 4000–525  $\text{cm}^{-1}$  with a spectrum resolution of 4  $\text{cm}^{-1}$ . All spectra were averaged over 32 scans.

**General procedure for the synthesis of aromatic oximes (2a, 2b, 2c, 2d, 2e, 2f, 2g):<sup>1</sup>**



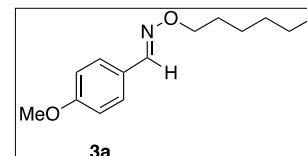
To a suspension of 20 mmol of the corresponding aldehyde (**1a-1g**) in a 3:1 mixture of H<sub>2</sub>O/EtOH (20 mL) was added hydroxylamine hydrochloride (20 mmol, 1.39 g), followed by 4 mL of a 50% aqueous solution of NaOH (40 mmol), while keeping the temperature below 30°C. After being stirred at room temperature for 2 hours, the solution was extracted with ethyl acetate. The aqueous phase was acidified to pH 6 by adding concentrated HCl and extracted with ethyl acetate. The combined organic phases were dried over Na<sub>2</sub>SO<sub>4</sub>, and the solvent was evaporated to give quantitatively the oxime product, which was used without further purification.

**General procedure for the synthesis of aromatic oxime ethers (3a, 3b, 3c, 3d, 3e, 3f, 2g, 3h, 3i):<sup>2</sup>**

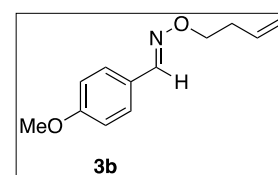


To a solution of the corresponding oxime (**2a-2g**, 6.61 mmol) and K<sub>2</sub>CO<sub>3</sub> (18.5 mmol, 2.56 g) in acetone (45 ml), the corresponding alkyl-bromide was added (9.91 mmol). The system was left under stirring to reflux for 16 hours, then the crude product was filtered. In the resulting solution, water was added, it was acidified till pH=7 and was extracted with ethyl acetate. The organic phase was dried with Na<sub>2</sub>SO<sub>4</sub> and the solvent was removed by rotary distillation. The obtained crude product was purified through chromatographic column and the obtainment of the desired compound was confirmed by elemental analysis and <sup>1</sup>H, <sup>13</sup>C and HSQC NMR analysis (spectra reported in the Supporting Information).

4-methoxybenzaldehyde *O*-hexyl oxime (**3a**, yield=62%): <sup>1</sup>H NMR (400.13 MHz, C<sub>6</sub>D<sub>6</sub>): δ 8.10 (s, 1H), 7.46 (d, J=8 Hz, 2H), 6.66 (d, J=8 Hz, 2H), 4.25 (t, J=8 Hz, 2H), 3.21 (s, 3H), 1.74 (qu, J=6 Hz, 2H), 1.37 (qu, J=6 Hz, 2H), 1.24 (m, 4H), 0.86 (t, J=8 Hz, 3H). <sup>13</sup>C NMR (100.61 MHz, C<sub>6</sub>D<sub>6</sub>): δ 161.2 (-C- arom.), 147.8 (-CH=N-O-), 128.7 (-CH- arom.), 125.9 (-C- arom.), 114.5 (-CH- arom.), 74.5 (=N-O-CH<sub>2</sub>-), 54.8 (-OCH<sub>3</sub>), 32.1 (-CH<sub>2</sub>-), 29.7 (-CH<sub>2</sub>-), 26.1 (-CH<sub>2</sub>-), 23.0 (-CH<sub>2</sub>-), 14.2 (-CH<sub>3</sub>). Anal. Calcd for C<sub>14</sub>H<sub>21</sub>NO<sub>2</sub>: C, 71.46; H, 9.00; N, 5.95. Found: C, 71.35; H, 9.01; N, 5.94.

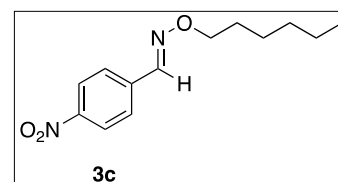


4-methoxybenzaldehyde *O*-(but-3-ene) oxime (**3b**, yield=59%): <sup>1</sup>H NMR (400 MHz, C<sub>6</sub>D<sub>6</sub>): δ 8.05 (s, 1H), 7.43 (d, J=8 Hz, 2H), 6.65 (d, J=8 Hz, 2H), 5.82 (m, 1H), 5.06 (m, 2H), 4.24 (t, J=8 Hz, 2H), 3.20 (s, 3H),

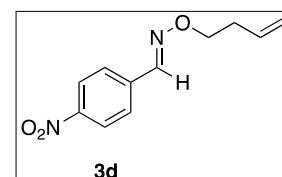


2.45 (qt,  $J_1=8$  Hz,  $J_2=2$ Hz, 3H).  $^{13}\text{C}$  NMR (100.61 MHz,  $\text{C}_6\text{D}_6$ ):  $\delta$  161.3 (-C- arom.), 148.2 (-CH=N-O-), 135.3 (-CH=), 128.8 (-CH- arom.), 125.7 (-C- arom.), 116.7 (=CH<sub>2</sub>), 114.5 (-CH- arom), 73.6 (=N-O-CH<sub>2</sub>-), 54.8 (-OCH<sub>3</sub>), 34.2 (-CH<sub>2</sub>-). Anal. Calcd for  $\text{C}_{12}\text{H}_{15}\text{NO}_2$ : C, 70.22; H, 7.37; N, 6.82. Found: C, 70.23; H, 7.37; N, 6.81.

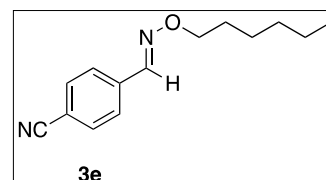
4-nitrobenzaldehyde *O*-hexyl oxime (**3c**, yield=87%):  $^1\text{H}$  NMR (400 MHz,  $\text{C}_6\text{D}_6$ ):  $\delta$  7.74 (d,  $J=8$  Hz, 2H), 7.73 (s, 1H), 7.09 (d,  $J=8$  Hz, 2H), 4.18 (t,  $J=8$  Hz, 2H), 1.66 (qu,  $J=6$  Hz, 2H), 1.27 (m, 6H), 0.87 (t,  $J=8$  Hz, 3H).  $^{13}\text{C}$  NMR (100.61 MHz,  $\text{C}_6\text{D}_6$ ):  $\delta$  148.4 (-C- arom.), 146.1 (-CH=N-O-), 138.6 (-C- arom.), 127.4 (-CH- arom.), 123.9 (-CH- arom.), 75.3 (=N-O-CH<sub>2</sub>-), 32.0 (-CH<sub>2</sub>-), 29.6 (-CH<sub>2</sub>-), 26.0 (-CH<sub>2</sub>-), 23.0 (-CH<sub>2</sub>-), 14.3 (-CH<sub>3</sub>). Anal. Calcd for  $\text{C}_{13}\text{H}_{18}\text{N}_2\text{O}_3$ : C, 62.38; H, 7.25; N, 11.19. Found: C, 62.17; H, 7.26; N, 11.16.



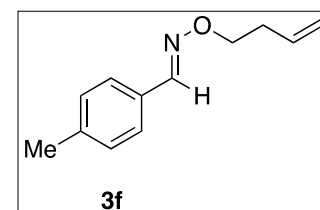
4-nitrobenzaldehyde *O*-(but-3-ene) oxime (**3d**, yield=85%):  $^1\text{H}$  NMR (400 MHz,  $\text{C}_6\text{D}_6$ ):  $\delta$  7.74 (d,  $J=8$  Hz, 2H), 7.68 (s, 1H), 7.08 (d,  $J=8$  Hz, 2H), 5.76 (m, 1H), 5.05 (m, 2H), 4.16 (t,  $J=8$  Hz, 2H), 2.37 (qt,  $J_1=8$  Hz,  $J_2=2$ Hz, 3H).  $^{13}\text{C}$  NMR (100.61 MHz,  $\text{C}_6\text{D}_6$ ):  $\delta$  148.5 (-C- arom.), 146.5 (-CH=N-O-), 138.3 (-C- arom.), 134.8 (-CH=), 127.4 (-CH- arom.), 123.9 (-CH- arom.), 117.0 (=CH<sub>2</sub>), 74.2 (=N-O-CH<sub>2</sub>-), 34.0 (-CH<sub>2</sub>-). Anal. Calcd for  $\text{C}_{11}\text{H}_{12}\text{N}_2\text{O}_3$ : C, 59.99; H, 5.49; N, 12.72. Found: C, 59.98; H, 5.50; N, 12.69.



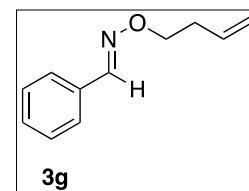
4-cyanobenzaldehyde *O*-hexyl oxime (**3e**, yield=81%):  $^1\text{H}$  NMR (400 MHz,  $\text{C}_6\text{D}_6$ ):  $\delta$  7.71 (s, 1H), 7.01 (d,  $J=8$  Hz, 2H), 6.85 (d,  $J=8$  Hz, 2H), 4.18 (t,  $J=8$  Hz, 2H), 1.66 (m, 2H), 1.28 (m, 6H), 0.87 (t,  $J=8$  Hz, 3H).  $^{13}\text{C}$  NMR (100.61 MHz,  $\text{C}_6\text{D}_6$ ):  $\delta$  146.5 (-CH=N-O-), 136.6 (-C- arom.), 132.3 (-CH- arom.), 127.2 (-CH- arom.), 118.5 (-CN), 113.3 (C arom.), 75.2 (=N-O-CH<sub>2</sub>-), 31.2 (-CH<sub>2</sub>-), 29.5 (-CH<sub>2</sub>-), 26.0 (-CH<sub>2</sub>-), 23.0 (-CH<sub>2</sub>-), 14.2 (CH<sub>3</sub>). Anal. Calcd for  $\text{C}_{14}\text{H}_{18}\text{N}_2\text{O}$ : C, 73.01; H, 7.88; N, 12.16. Found: C, 73.02; H, 7.89; N, 12.16.



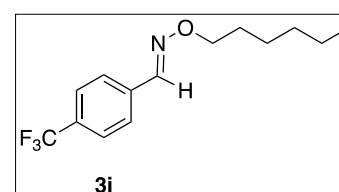
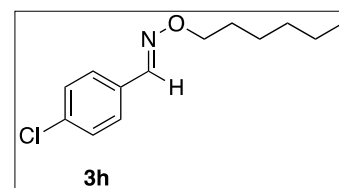
4-methylbenzaldehyde *O*-buten oxime (**3f**, yield=53%):  $^1\text{H}$  NMR (400 MHz,  $\text{C}_6\text{D}_6$ ):  $\delta$  8.07 (s, 1H), 7.43 (d,  $J=8$  Hz, 2H), 6.87 (d,  $J=8$  Hz, 2H), 5.81 (m, 1H), 5.05 (m, 2H), 4.24 (t,  $J=8$  Hz, 2H), 2.44 (qt,  $J_1=8$  Hz,  $J_2=2$ Hz, 3H), 2.00 (s, 3H).  $^{13}\text{C}$  NMR (100.61 MHz,  $\text{C}_6\text{D}_6$ ):  $\delta$  148.5 (-CH=N-O-), 139.8 (-C- arom.), 135.3 (-CH=), 130.4 (-CH- arom.), 129.6 (-C- arom.), 127.3 (-C- arom.), 116.7 (=CH<sub>2</sub>), 73.6 (=N-O-CH<sub>2</sub>-), 34.2 (-CH<sub>2</sub>-), 21.3 (-CH<sub>3</sub>). Anal. Calcd for  $\text{C}_{12}\text{H}_{15}\text{NO}$ : C, 76.16; H, 7.99; N, 7.40. Found: C, 76.02; H, 8.01; N, 7.38.



benzaldehyde *O*-buten oxime (**3g**, yield=55%):  $^1\text{H}$  NMR (400 MHz,  $\text{C}_6\text{D}_6$ ):  $\delta$  8.01 (s, 1H), 7.45 (d,  $J=8$  Hz, 2H), 7.02 (d,  $J=8$  Hz, 2H), 5.80 (m, 1H), 5.05 (m, 2H), 4.22 (t,  $J=8$  Hz, 2H), 2.42 (qt,  $J_1=8$  Hz,  $J_2=2$ Hz, 3H).  $^{13}\text{C}$  NMR (100.61 MHz,  $\text{C}_6\text{D}_6$ ):  $\delta$  148.5 (-CH=N-O-), 135.2 (-C- arom.), 133.1 (-CH=), 130.4 (-CH- arom.), 129.7 (-C- arom.), 127.3 (-C- arom.), 116.7 (=CH<sub>2</sub>), 73.7 (=N-O-CH<sub>2</sub>-), 34.1 (-CH<sub>2</sub>-). Anal. Calcd for  $\text{C}_{11}\text{H}_{13}\text{NO}$ : C, 75.40; H, 7.48; N, 7.99. Found: C, 75.22; H, 7.49; N, 7.96.



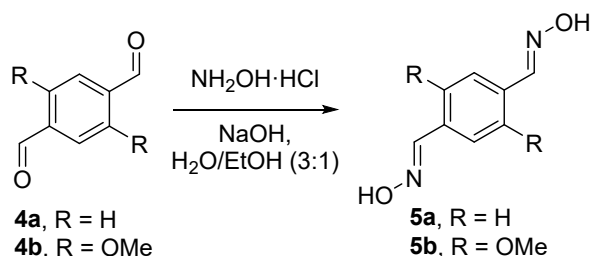
4-chlorobenzaldehyde *O*-hexyl oxime (**3h**, yield=62%):  $^1\text{H}$  NMR (400 MHz,  $\text{C}_6\text{D}_6$ ):  $\delta$  7.86 (s, 1H), 7.16 (d,  $J=8$  Hz, 2H), 6.98 (d,  $J=8$  Hz, 2H), 4.20 (t,  $J=8$  Hz, 2H), 1.69 (qu,  $J=6$  Hz, 2H), 1.34 (qu,  $J=6$  Hz, 2H), 1.23 (m, 4H), 0.86 (t,  $J=8$  Hz, 3H).  $^{13}\text{C}$  NMR (100.61 MHz,  $\text{C}_6\text{D}_6$ ):  $\delta$  146.9 (-C- arom.), 146.8 (-CH=N-O-), 135.5.7 (-C- arom.), 131.6 (-CH- arom.), 129.1 (-CH- arom.), 74.8 (=N-O-CH<sub>2</sub>-), 32.1 (-CH<sub>2</sub>-), 29.7 (-CH<sub>2</sub>-), 26.1 (-CH<sub>2</sub>-), 23.1 (-CH<sub>2</sub>-), 14.3 (-CH<sub>3</sub>). Anal. Calcd for  $\text{C}_{13}\text{H}_{18}\text{ClNO}$ : C, 65.13; H, 7.57; N, 5.84. Found: C, 64.92; H, 7.60; N, 5.83.



4-(trifluoromethyl)benzaldehyde *O*-hexyl oxime (**3i**, yield=62%): <sup>1</sup>H NMR (400 MHz, C<sub>6</sub>D<sub>6</sub>): δ 7.85 (s, 1H), 7.23 (m, 4H), 4.21 (t, J=8 Hz, 2H), 1.69 (qu, J=6 Hz, 2H), 1.29 (m, 6H), 0.87 (t, J=8 Hz, 3H). <sup>13</sup>C NMR (100.61 MHz, C<sub>6</sub>D<sub>6</sub>): δ 146.8 (-CH=N-O-), 136.4 (-C- arom.), 131.2 (q, J=30 Hz, -C-CF<sub>3</sub>), 127.3 (-CH- arom.), 125.7 (q, J=4 Hz, -CH- arom.), 124.9 (q, J=270 Hz, -CF<sub>3</sub>), 75.1 (=N-O-CH<sub>2</sub>-), 32.0 (-CH<sub>2</sub>-), 29.6 (-CH<sub>2</sub>-), 26.0 (-CH<sub>2</sub>-), 23.1 (-CH<sub>2</sub>-), 14.3 (-CH<sub>3</sub>). Anal. Calcd for C<sub>14</sub>H<sub>18</sub>F<sub>3</sub>NO: C, 61.53; H, 6.64; N, 5.13. Found: C, 61.58; H, 6.66; N, 5.12.

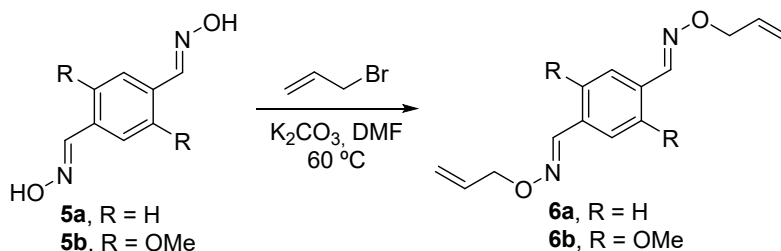
- Representative example for oxime-ethers model reaction: 4-methoxybenzaldehyde *O*-(but-3-ene) oxime (**3b**) (0.49 mmol, 100 mg), 4-nitrobenzaldehyde *O*-hexyl oxime (**3e**) (0.49 mmol, 121 mg) and para-toluensulfonic acid (0.05 mmol, 9.5 mg) were mixed in vial and heated to 100 °C. The reaction was monitored with <sup>1</sup>H NMR, by sampling the reaction crude every 15, 30, 60, 120, 180 and 480 minutes.

### Synthesis of terephthalaldehyde dioximes (5a-b):<sup>1</sup>



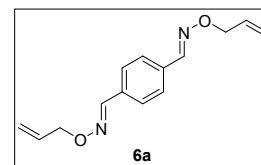
To a suspension of the corresponding terephthalaldehyde **4** (20 mmol) in a 3:1 mixture of H<sub>2</sub>O/EtOH (20 mL) was added hydroxylamine hydrochloride (40 mmol), followed by 8 mL of a 50% aqueous solution of NaOH (80 mmol), while keeping the temperature below 30 °C. After being stirred at room temperature for 2 hours, the solution was extracted with ethyl acetate. The aqueous phase was acidified to pH 6 by adding concentrated HCl and extracted with ethyl acetate. The combined organic phases were dried over Na<sub>2</sub>SO<sub>4</sub>, and the solvent was evaporated to give quantitatively the terephthalaldehyde oxime **5**, which was used without further purification.

### Synthesis of terephthalaldehyde *O*-(prop-2-ene) dioximes (6a-b):<sup>2</sup>

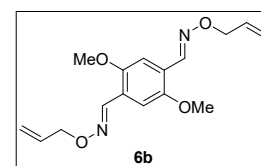


To a solution of dioxime **5** (6.61 mmol) and K<sub>2</sub>CO<sub>3</sub> (18.5 mmol, 2.56 g) in DMF (25 ml), 3-bromo-1-propene (19.8 mmol) was added. The system was left stirring at 60 °C for 16 hours, then the crude product was filtered. The resulting solution was purified through chromatographic column and the obtainment of the desired compound, with a yield of 92% (**6a**) and 85 % (**6b**). The oximes were characterized by elemental analysis and <sup>1</sup>H, <sup>13</sup>C and HSQC NMR analysis.

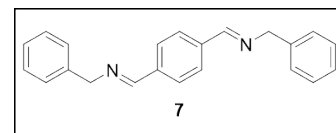
terephthalaldehyde *O*-(prop-2-ene) dioxime (**6a**, yield=92%): <sup>1</sup>H NMR (400 MHz, C<sub>6</sub>D<sub>6</sub>): δ 7.91 (s, 2H), 7.34 (s, 4H), 5.97 (m, 2H), 5.16 (m, 4H), 4.63 (dt, J<sub>1</sub>=6 Hz, J<sub>2</sub>=2 Hz, 4H). <sup>13</sup>C NMR (100.61 MHz, C<sub>6</sub>D<sub>6</sub>): δ 148.3 (-CH=N-O-), 134.7 (-CH=), 134.0 (C arom.), 127.6 (CH arom.), 117.6 (=CH<sub>2</sub>), 75.5 (=N-O-CH<sub>2</sub>-). Anal. Calcd for C<sub>14</sub>H<sub>16</sub>N<sub>2</sub>O<sub>2</sub>: C, 68.83; H, 6.60; N, 11.47. Found: C, 68.79; H, 6.62; N, 11.44.



terephthalaldehyde *O*-(prop-2-ene) dioxime (**6b**, yield=85%): <sup>1</sup>H NMR (400 MHz, CDCl<sub>3</sub>): δ 8.48 (s, 2H), 7.33 (s, 2H), 6.05 (dq, J = 17.3, 10.4 Hz, 2H), 5.29 (ddq, J = 17.3, 1.6 Hz, 2H, 4H), 4.69 (dt, J = 5.7, 1.4 Hz, 4H) 3.84 (s, 6H). <sup>13</sup>C NMR (100.61 MHz, CDCl<sub>3</sub>): δ 151.9 (-CH=N-O-), 144.7 (-CH=), 134.2 (C arom.), 123.1 (CH arom.), 117.9 (=CH<sub>2</sub>), 108.6 (CH arom.), 75.3 (=N-O-CH<sub>2</sub>-), 56.3 (-O-CH<sub>3</sub>).



1,1'-(1,4-phenylene)bis(N-benzylmethanimine) (**7**, yield=100%): Terephthalaldehyde (565 mg, 4.22 mmol) and benzylamine (904 mg, 8.44 mmol) were mixed in a vial and stirred open



air at 120 °C for 3h. <sup>1</sup>H NMR (400 MHz, CDCl<sub>3</sub>): δ 8.42 (t, *J*=1.4 Hz, 2H), 7.83 (s, 4H), 7.36 (m, 10H), 4.85 (s, 4H).

## MOLECULAR MODEL REACTIONS

***Kinetic experiments for oxime exchange:*** General procedure. Representative oxime **3b** and **3c** were equimolarly mixed (0.5 mmol) in a vial. When applicable, a 10 % wt of catalyst was added and the vial was stirred at 100 °C. At different reaction times, aliquots were taken and the mixture was dissolved in C<sub>6</sub>D<sub>6</sub> for NMR analysis.

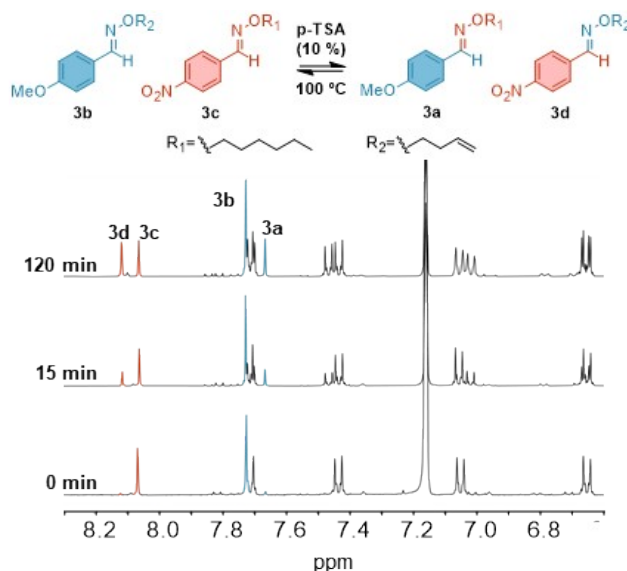


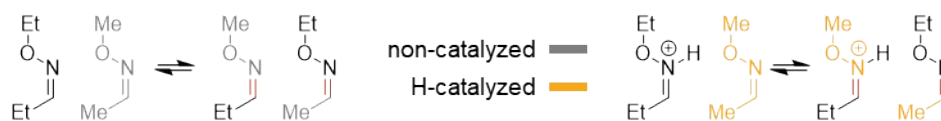
**Figure S1.** Metathesis reaction of compounds **3b** and **3c** and the corresponding magnification (8.5-6.5 ppm) of <sup>1</sup>H-NMR spectra (C<sub>6</sub>D<sub>6</sub>, 400 MHz) of the oxime metathesis reaction.

## COMPUTATIONAL METHODS

Ab-initio density functional theory (DFT) calculations have been performed using the Orca code version 5.02.<sup>4</sup> The preparatory calculations such as conformer search and location of plausible transition states has been done using the Crest tool relying on the GFN2-xTB (xTB) semi-empirical method and the GNF-FF (GFF) force field.<sup>5-8</sup>

In order to assess the mechanism, we initially explored the reactivity on a model system made by two asymmetric oximes with simple aliphatic substituents (see Scheme 1). The reaction path by means of two methods: a first set of preliminary calculations was done using the relatively fast PBEh-3c method;<sup>9</sup> these were then repeated using B3LYP with a Def2-TZVP basis set and D3BJ dispersion corrections.<sup>10</sup> All geometries were characterized by a harmonic frequency calculation to ensure we were dealing with the correct kind of stationary point, e.g., minima or first-order saddle points. The evaluation of the Hessian has allowed us to compute the zero-point-energy (ZPE) corrected electronic energies and the Gibbs free energies associated with each geometry. No solvent or environmental effects have been included.

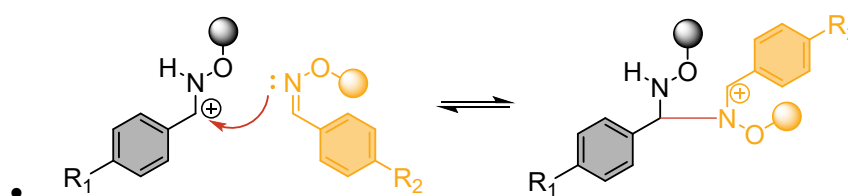
The system chosen to explore the reaction mechanisms contains the compounds illustrated in Scheme 1. We have calculated the reaction path in both a neutral system (Scheme 1, on the left) and in a protonated one where the nitrogen atom is protonated (Scheme 1, on the right).



**Scheme S1:** Model systems used to explore the reaction mechanism in the computational study. Left: neutral system. Right: protonated system

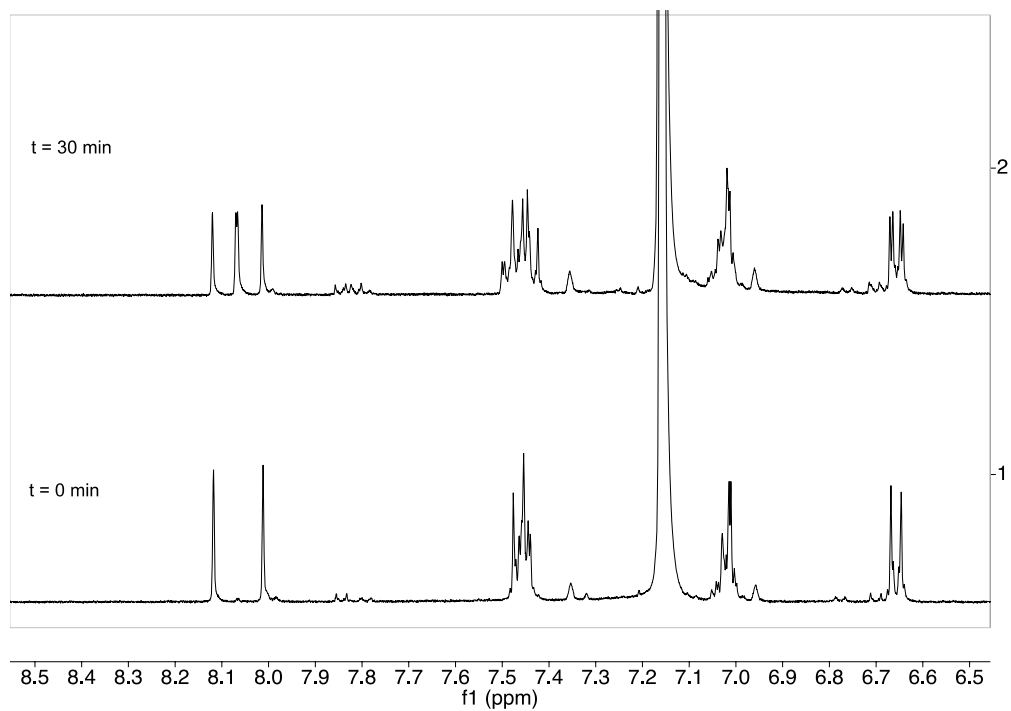
The calculations on the experimental systems have been done in a more complex way. The molecules at hand present a very large conformational freedom due to the chains on the aromatic rings and, especially in the pre- and post-reaction complexes due to possible intermolecular interactions such as hydrogen bonding and pi-pi stacking. The procedure we have used depends whether we wanted a candidate for the transition state or for the intermediates and is the following:

- The lowest energy conformers of the isolated reactants, isolated products, pre-reaction complex, cyclic intermediate and post-reaction complex have been found using the conformational search algorithm in the Crest tool using the GFF force field. The lowest 100 conformers have then been reoptimized using xTB. A suitable candidate for the absolute minima was then selected as the lowest-energy xTB structure found. This candidate has been selected for further DFT optimization. Given the size of the molecular structures the optimization and frequency evaluation has been done using the R<sup>2</sup>scan-3c method which guarantees an accuracy comparable to hybrid-DFT/QZ methods, but at a fraction of the cost.<sup>11</sup>
- Plausible initial geometries for the transition states have been generated using the NEB algorithm within Orca employing the xTB semi empirical method.<sup>12</sup> The candidate transition states have then been reoptimized and treated with R<sup>2</sup>Scan-3c as above.

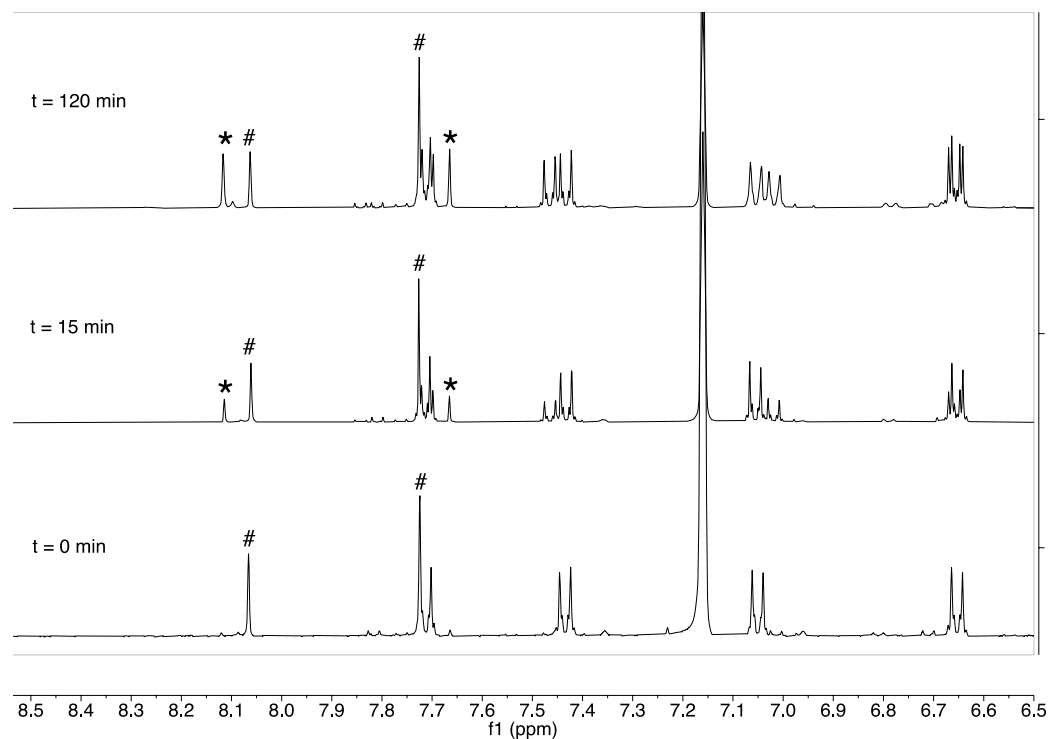


- **Scheme S2.** Rate-determining step for the proposed acid-catalyzed oxime metathesis mechanism.

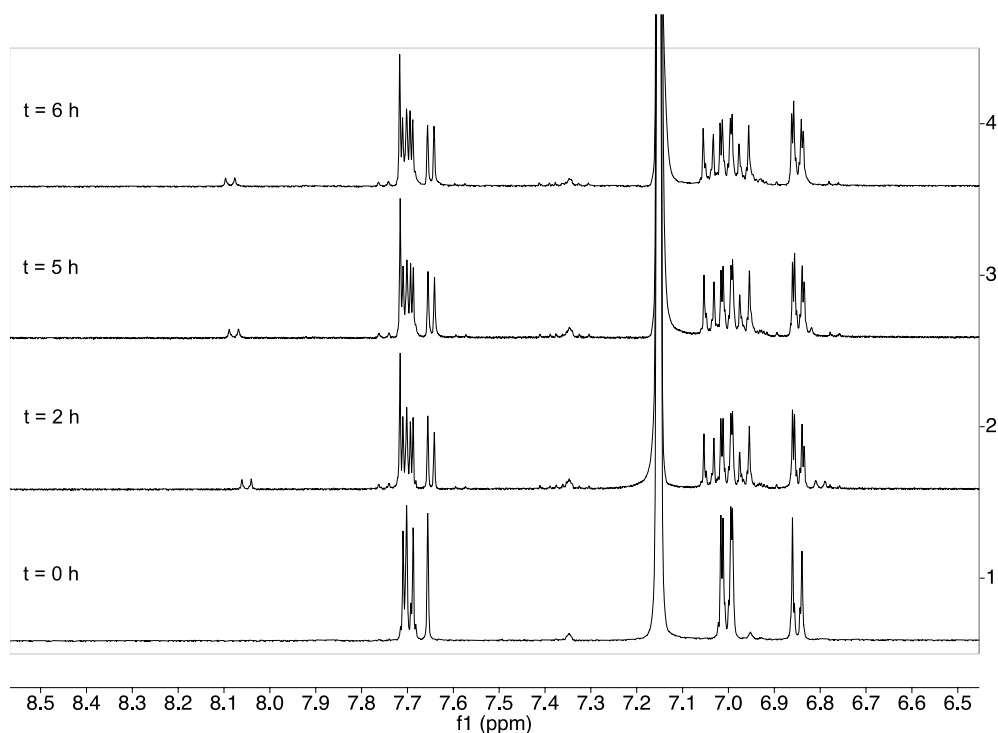
## SUBSTITUENT EFFECT STUDY



- **Figure S2.** Magnification (8.5-6.5 ppm) of the  $^1\text{H}$  NMR spectra of the metathesis reaction between benzaldehyde *O*-(but-3-ene) oxime (**3g**) and 4-methoxybenzaldehyde *O*-hexyl oxime (**3a**) (EDG-EDG).



- **Figure S3.** Magnification (8.5-6.5 ppm) of the  $^1\text{H}$  NMR spectra of the metathesis reaction between 4-nitrobenzaldehyde *O*-hexyl oxime (**3c**) and 4-methoxybenzaldehyde *O*-(but-3-ene) oxime (**3b**) (EWG-EDG)



- **Figure S4.** Magnification (8.5-6.5 ppm) of the  $^1\text{H}$  NMR spectra of the metathesis reaction 4-nitrobenzaldehyde *O*-(but-3-ene) oxime (**3d**) and 4-cyanobenzaldehyde *O*-hexyl oxime (**3e**) (EWG-EWG)

In order to characterize the entire reaction path, we report here both the  $\text{R}^2\text{scan-3c}$  Gibbs free energies (thus including ZPE, thermal corrections and entropy) and the electronic energy with no corrections. The reaction profile has been computed for two exemplar systems (EWG-EWG, EDG-EDG) for both possible nitrogen protonation states. The calculations of the reaction paths for the neutral system have not been carried out, due to the results obtained on the model system. As before, no environmental or solvent effects have been included.

**Table S1:**  $\text{R}^2\text{scan-3c}$  relative Gibbs free energies (kcal/mol) of the reactions for the 4 protonated systems. The same data are displayed in Figures S5.

Protonation	$\text{H}^+$ long alkyl chain		$\text{H}^+$ short alkyl chain	
	$-\text{NO}_2/-\text{CF}_3$	$-\text{Me}/-\text{OMe}$	$-\text{NO}_2/-\text{CF}_3$	$-\text{Me}/-\text{OMe}$
<b>Pre-react. complex</b>	-6.2	-4.5	0.8	4.6
<b>#TS1</b>	36.0	30.2	26.5	26.0
<b>Cycle</b>	27.1	19.8	24.7	16.2
<b>#TS2</b>	34.2	28.4	31.0	28.3
<b>Post-react. complex</b>	1.5	-2.3	-3.0	-7.6

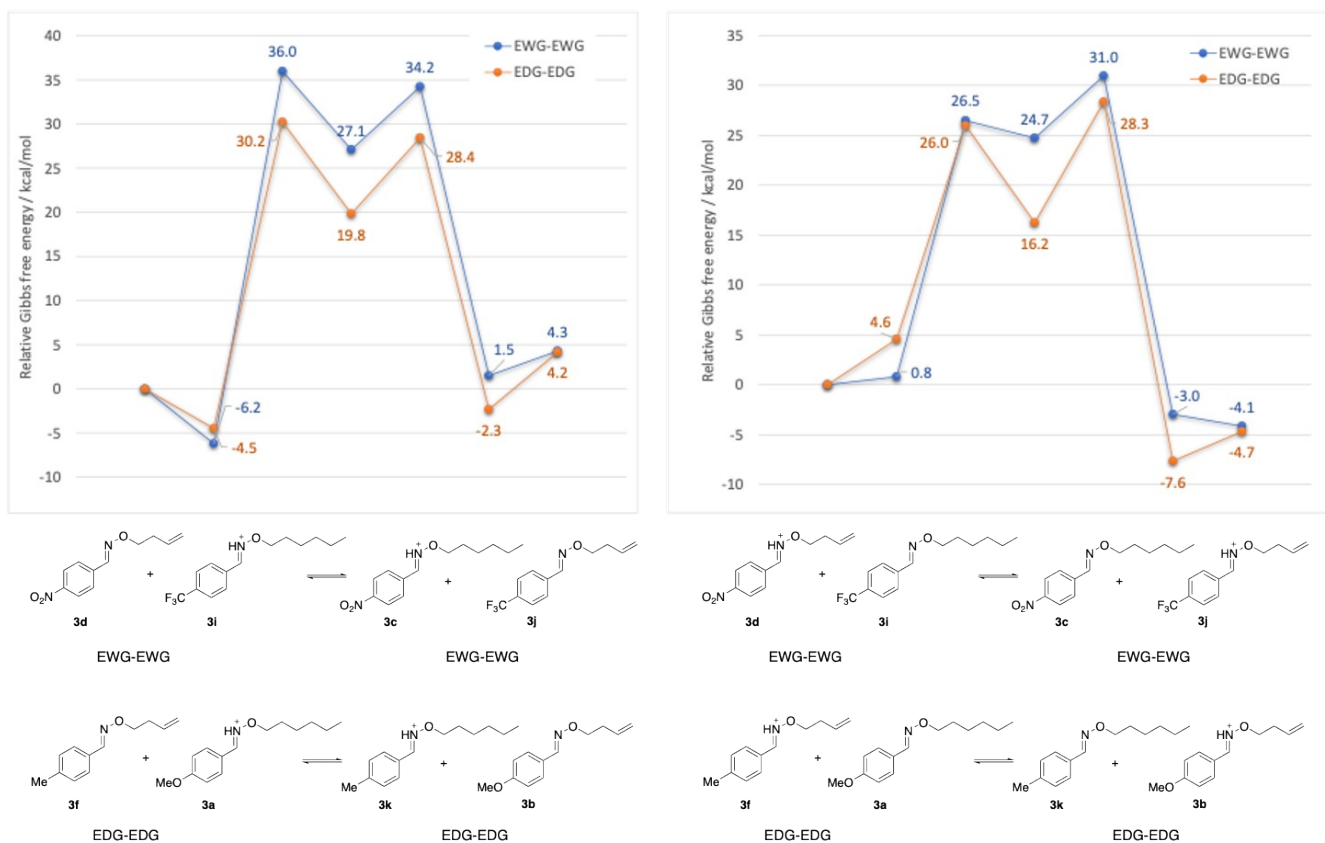


**Figure S5:** R<sup>2</sup>scan-3c Gibbs free energy of the reactions for the protonated systems. Left and right panels differ for the position of the proton. The energies, from left to right, pertain to: isolated reactants, reactant complex, first transition state, cyclic intermediate, second transition state, product complex, isolated products. The energy of the isolated reactants has been chosen as the zero of the energy scale.

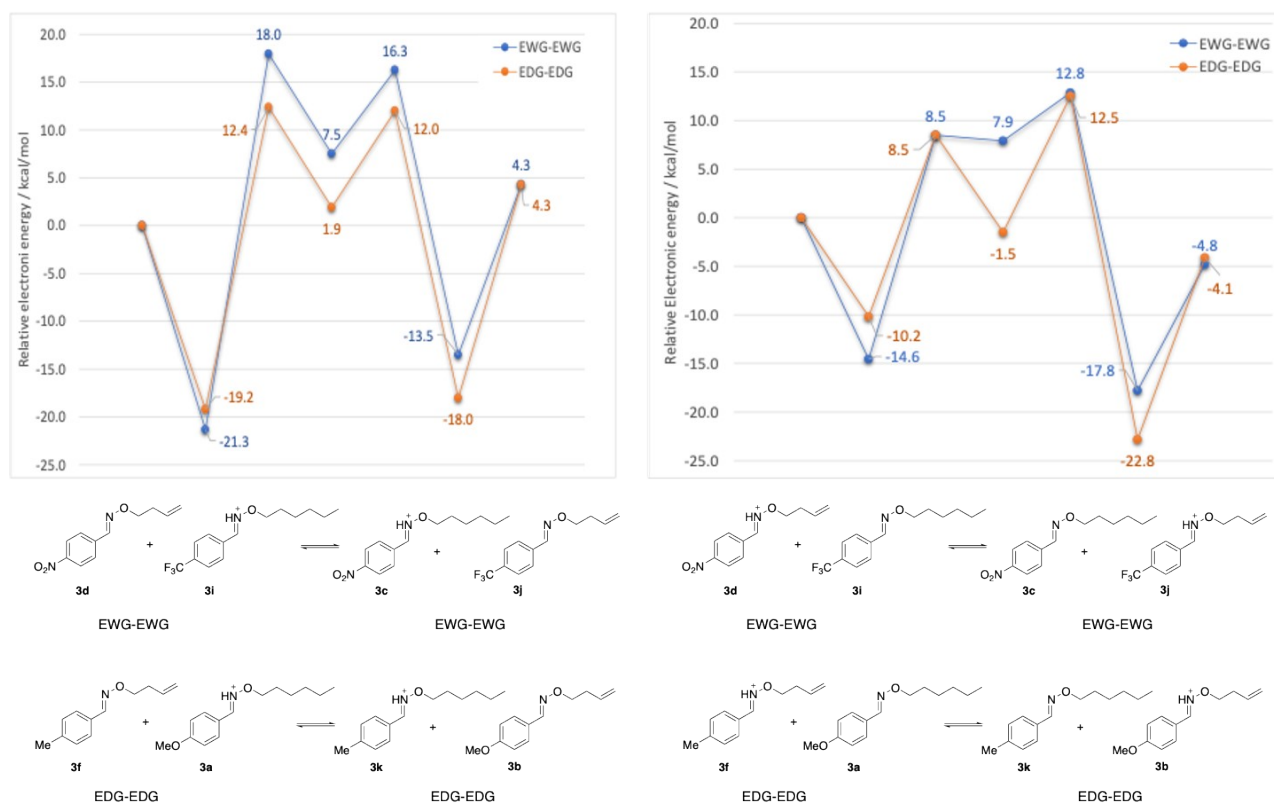


**Figure S6:** R<sup>2</sup>scan-3c electronic energy of the reactions for the protonated systems. Left and right panels differ for the position of the proton. The energies, from left to right, pertain to: isolated reactants, reactant complex, first transition state,

cyclic intermediate, second transition state, product complex, isolated products. The energy of the isolated reactants has been chosen as the zero of the energy scale.

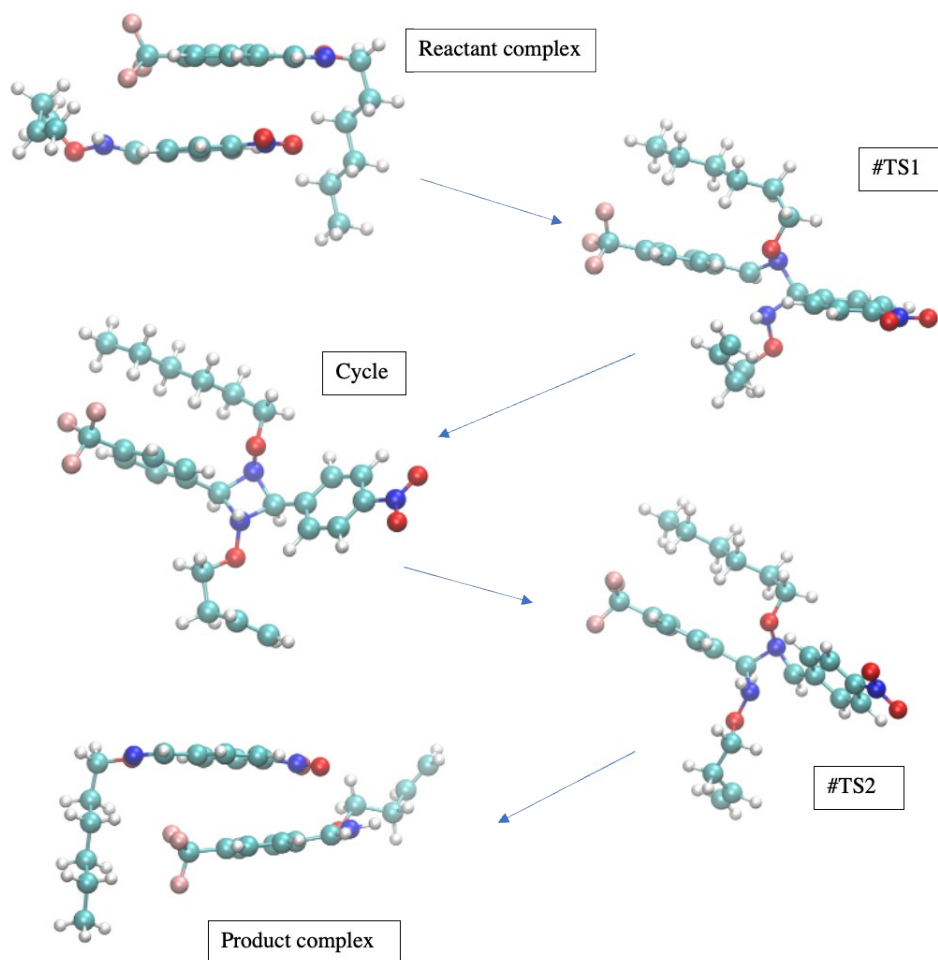


**Figure S7:** Geometries along the reaction path (EWG-EWG, protonation on the oxime bearing the -NO<sub>2</sub> group).



**Figure S8.** Summary of the computational results reported in Figure S5. Gibbs free energy relative to the isolated reactants of the reactions between oxime pair **3d/3i** and between oxime pair **3f/3a** for the protonated systems.

## HYDROLYTIC STABILITY: IMINES VS OXIMES

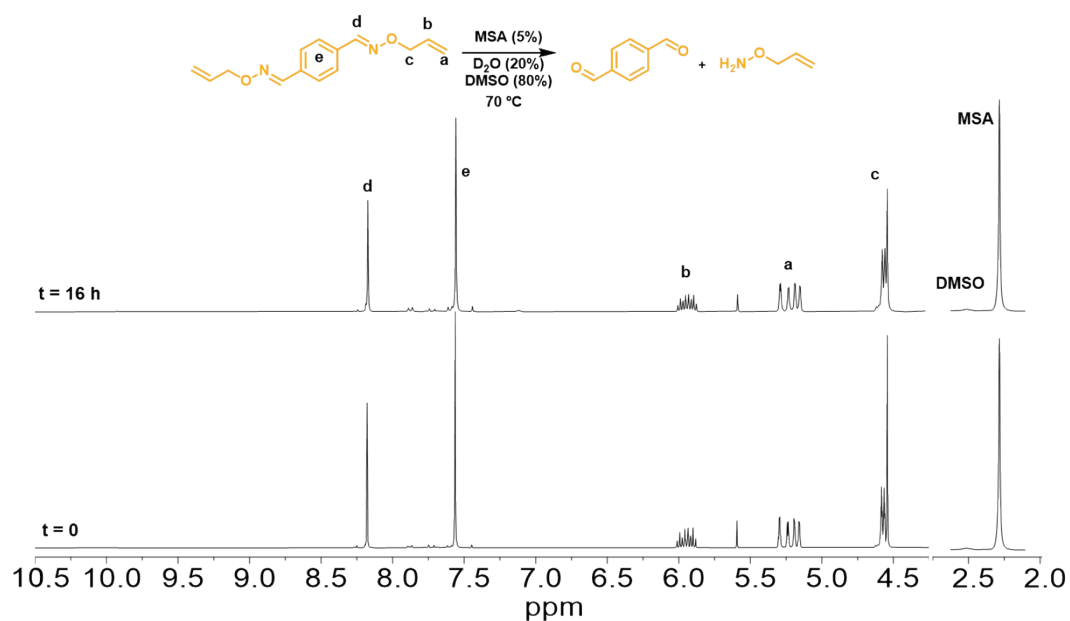


**Figure S9.** Spectrum of dioxime 6a in DMSO:D<sub>2</sub>O (8:2) in presence of 5% of MSA. No hydrolysis is observed after 16h at 70 °C.

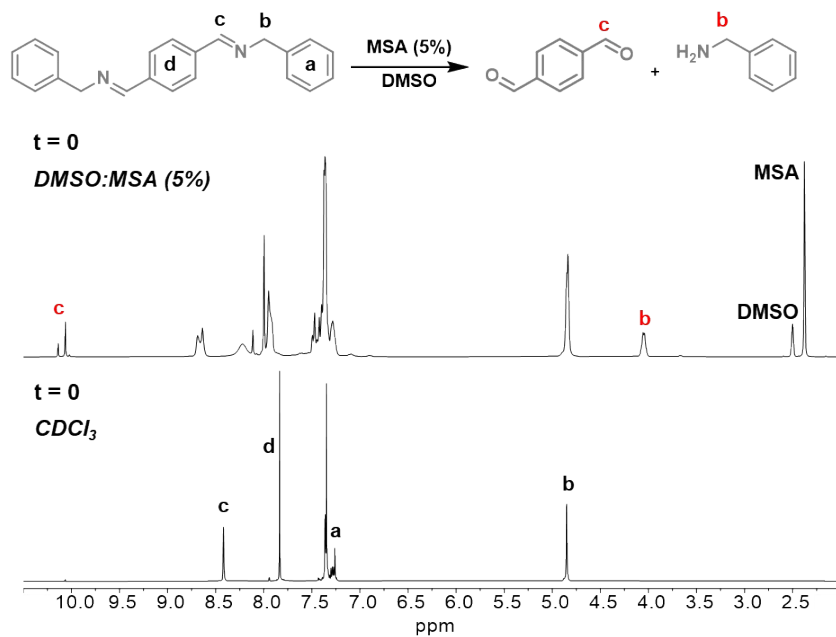


**Figure S10.** Spectrum of 7 in CDCl<sub>3</sub> (bottom) versus DMSO-*d*<sub>6</sub> with 5% of MSA. Partial imine cleavage is observed at room temperature.

## NETWORK CROSSLINKING

### Synthesis of PTE-DOx:

Dioxime **6a** (400 mg, 1.64 mmol), trimethylolpropanetris(3-mercaptopropionate) (**TPTM**) (217.5 mg, 0.55 mmol) and 1,6 hexanedithiol (**HDT**) (123.1 mg, 0.82 mmol) were mixed in a vial, stirred and heated to 60 °C until complete homogenization of the mixture. In a second vial, Irgacure 819 (8 mg, 1 %) and methanesulfonic acid (14.4 mg, 0.15 mmol) were dissolved in 50  $\mu\text{L}$  of acetone, then added to the previous mixture and stirred. The mixture was transferred to a circular Teflon mold and placed under a UV lamp ( $\lambda = 385 \text{ nm}$ , intensity =  $1 \text{ mW/cm}^2$ ) for 30 minutes. The resulting film was postcured at 110 °C for 30 min.

### Synthesis of PTE-DOx-OMe:

Dioxime **6a** (300 mg, 1.23 mmol), dioxime **6b** (93.4 mg, 0.31 mmol), trimethylolpropanetris(3-mercaptopropionate) (**TPTM**) (203.9 mg, 0.51 mmol) and 1,6 hexanedithiol (**HDT**) (115.4 mg, 0.77 mmol) were dissolved in a vial with 250  $\mu\text{L}$  of acetone, stirred and heated to 60 °C. In a second vial, camphorquinone (7 mg, 1 %) and methanesulfonic acid (13.5 mg, 0.14 mmol) were dissolved in 50  $\mu\text{L}$  of acetone, then added to the previous mixture and stirred. The mixture was transferred to a circular Teflon mold and placed under a UV lamp ( $\lambda = 467 \text{ nm}$ , intensity =  $1 \text{ mW/cm}^2$ ) for 30 minutes. The resulting film was postcured at 110 °C for 30 min.

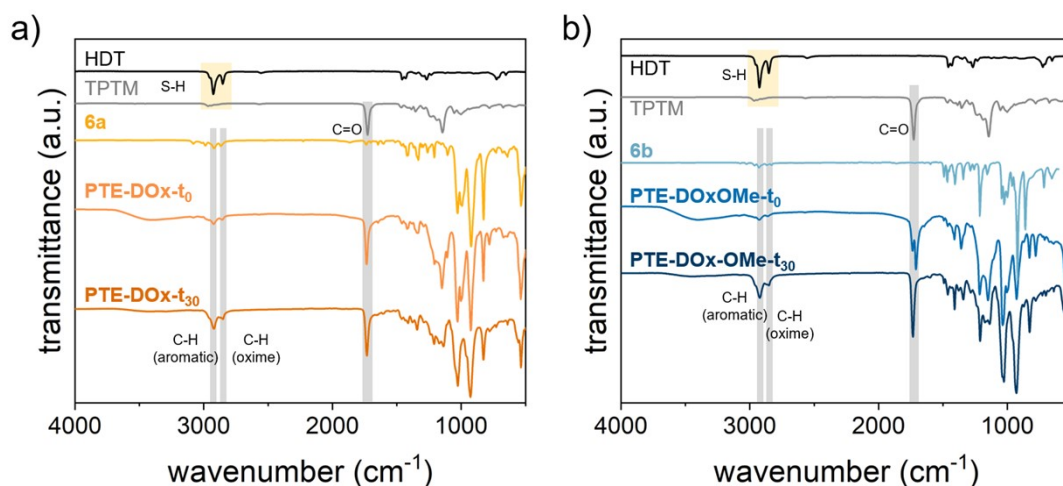


**Figure S11.** ATR-FTIR spectra of as-made PTE-DOx and PTE-DOx-OMe and the corresponding reprocessed materials

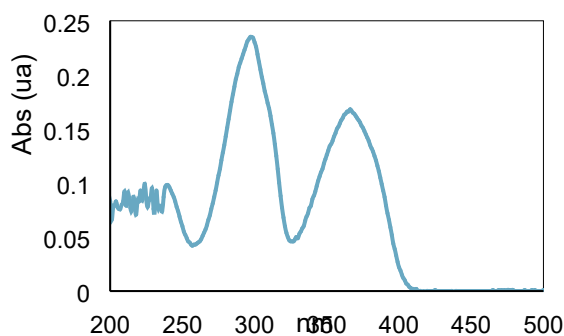


**Figure S12.** UV spectra of dioxime **6b**.

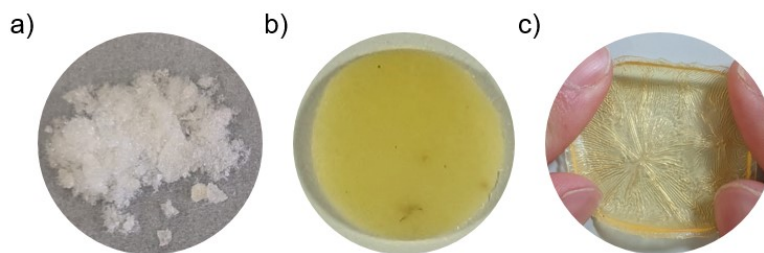


**Figure S13.** Visual appearance of a) dioxime monomer **6b**, b) PTE-DOx-OMe, bearing a 20 % of **6b**, c) attempt on the polymer with 50% content of **6b**.

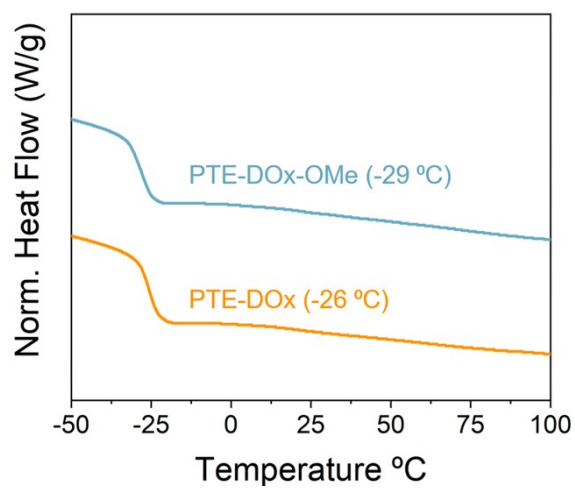


**Figure S14.** DSC curves for PTE-DOx and PTE-DOx-OMe. Values in parentheses represent the midpoints of T<sub>g</sub>.

## RHEOLOGICAL CHARACTERIZATION

Stress relaxation experiments to obtain the relaxation modulus  $E(t)$  were carried out in an ARES rheometer (Rheometrics) at different temperatures, using a film tension fixture and 1% of strain. Sample width between 3.0 and 4.0 mm was used, and a thickness between 0.2 and 0.4 mm. All samples were subjected to thermal stabilization at 150 °C for 15 min prior to measurement. For each sample, the temperature was varied in the range of 120 to 150 °C; before each measurement, the sample was allowed to thermally stabilize (5 minutes) at the target temperature. Activation energies were obtained following Arrhenius equation (1):

$$\ln \tau^*(T) = \ln \tau_0 + E_a / RT \quad (1)$$

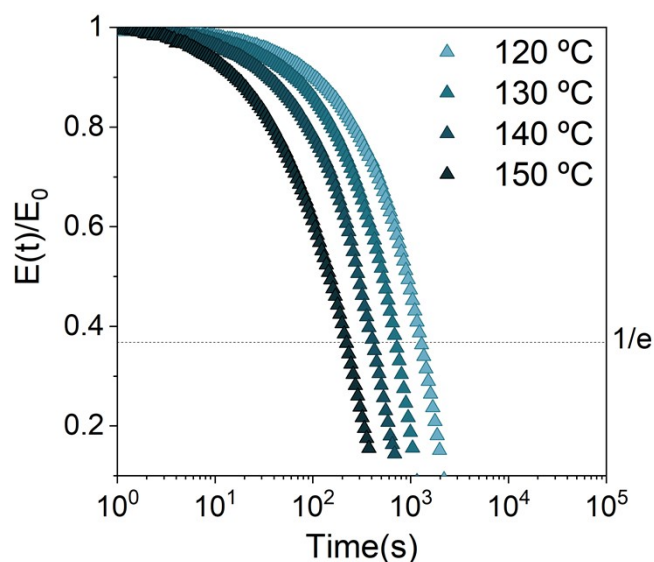


**Figure S15.** Normalized stress-relaxation curves performed at different temperatures PTE-DOx-OMe.

Small Amplitude Oscillatory shear experiments were performed at room temperature using a parallel plate geometry ( $\varnothing = 8$  mm) and under linear viscoelastic conditions for all the samples.

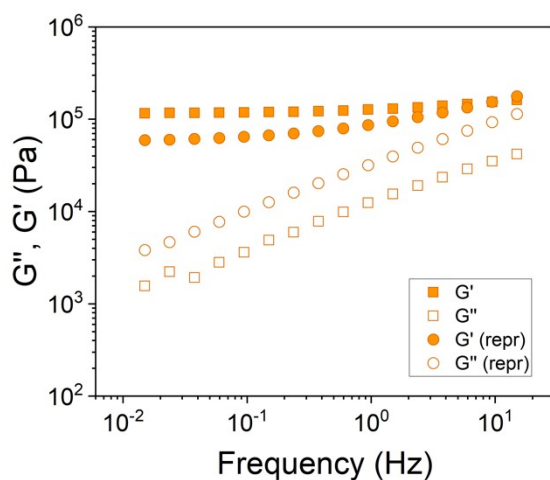


**Figure S16.**  $G'$  and  $G''$  vs frequency scans at room temperature for as-made and reprocessed PTE-DOx.

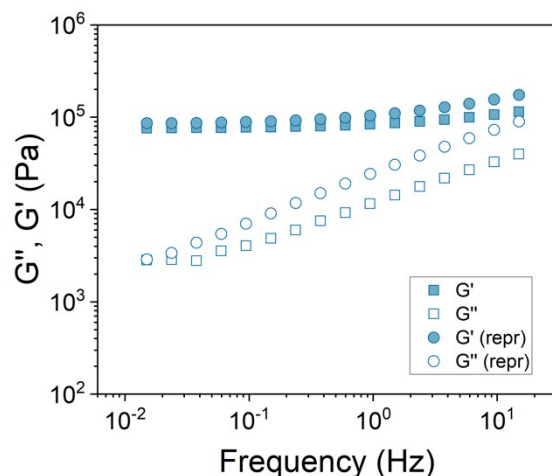


**Figure S17.**  $G'$  and  $G''$  vs frequency scans at room temperature for as-made PTE-DOx-OMe and the corresponding reprocessed material.

## REPROCESSING STUDIES

The dynamic network was cut into pieces with a razor blade ( $\sim 0.05$  g), and then placed into a circular mould (ca.  $d=10$  mm, 1 mm (T)) under a hot press ( $130$  °C, 9 kPa) covered with Teflon film for both sides for required periods of time. The mold was cooled to room temperature and the reprocessed samples were demoulded.

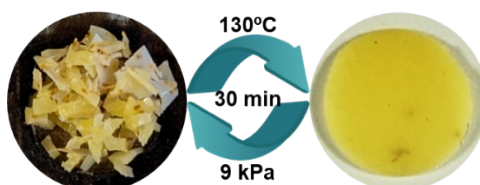


**Figure S18.** Visual appearance of PTE-DOx-OMe before and after reprocessing under hot pressing at  $130$  °C and 9kPa for 30 minutes.

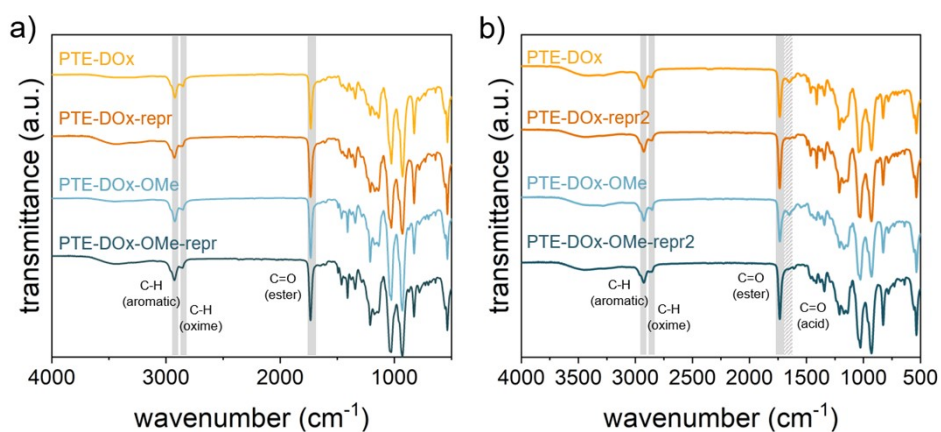


**Figure S19.** ATR-FTIR spectra of as-made PTE-DOx and PTE-DOx-OMe and the corresponding reprocessed materials (a) and the reprocessed materials for a 2n cycle (b).

## MR SPECTRA

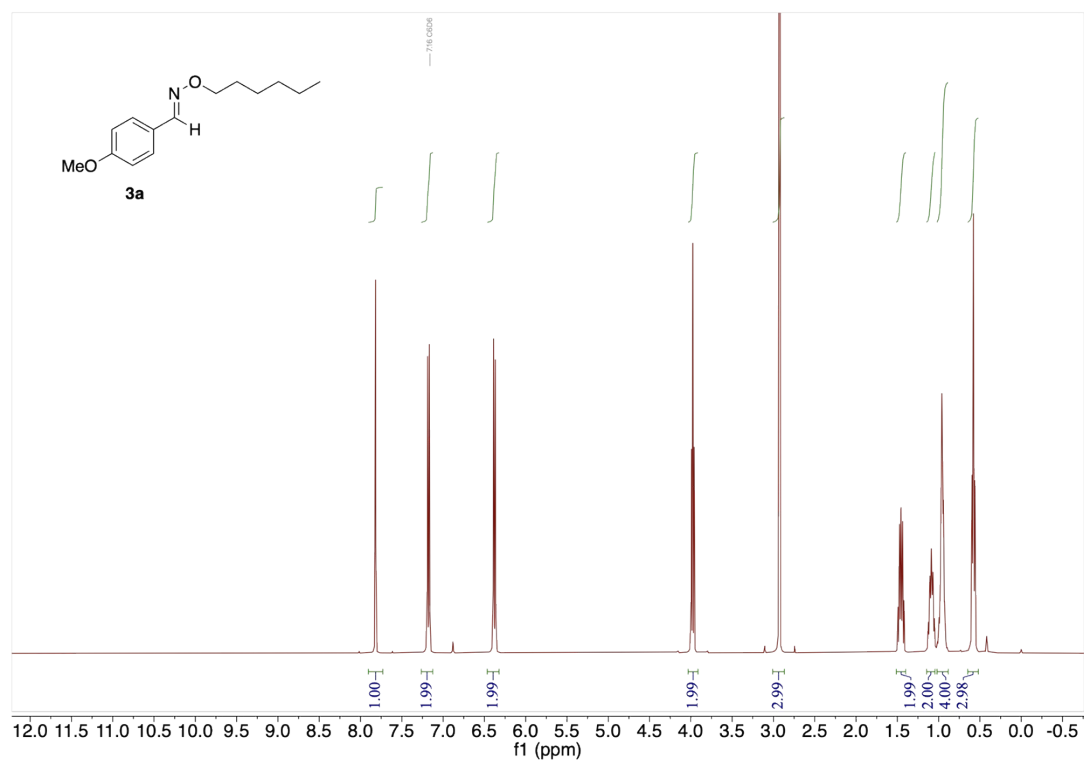


Figure S20. <sup>1</sup>H-NMR spectra of compound 3a

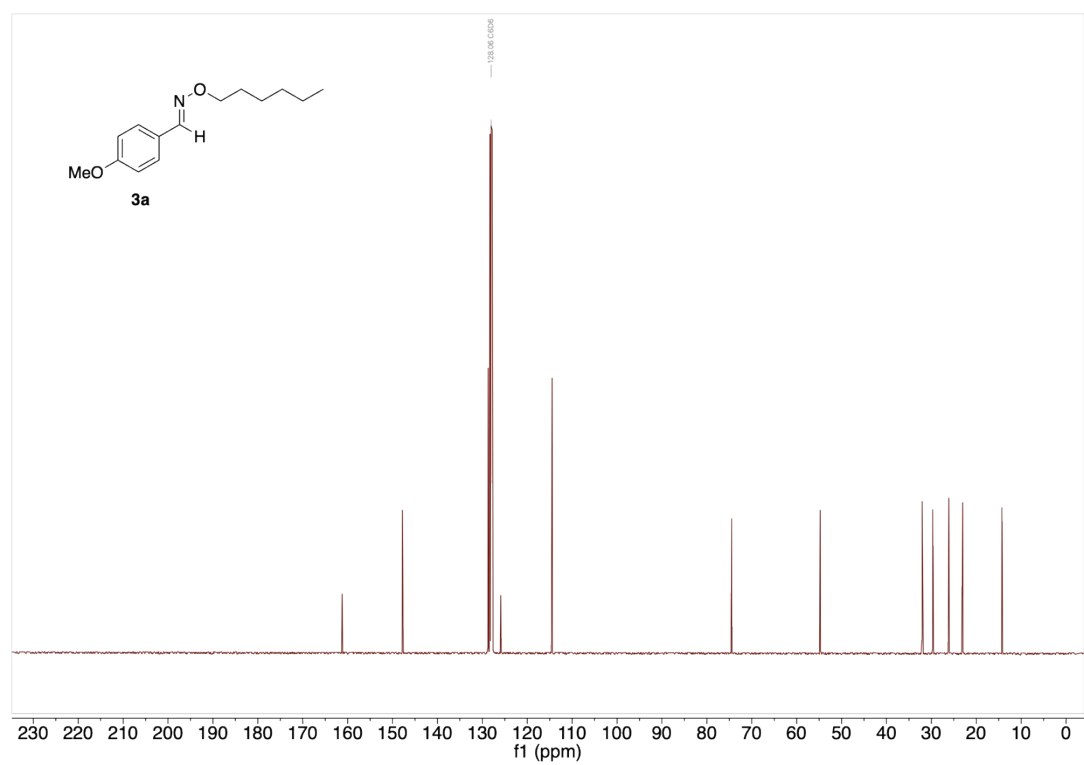


Figure S21. <sup>13</sup>C-NMR spectra of compound 3a

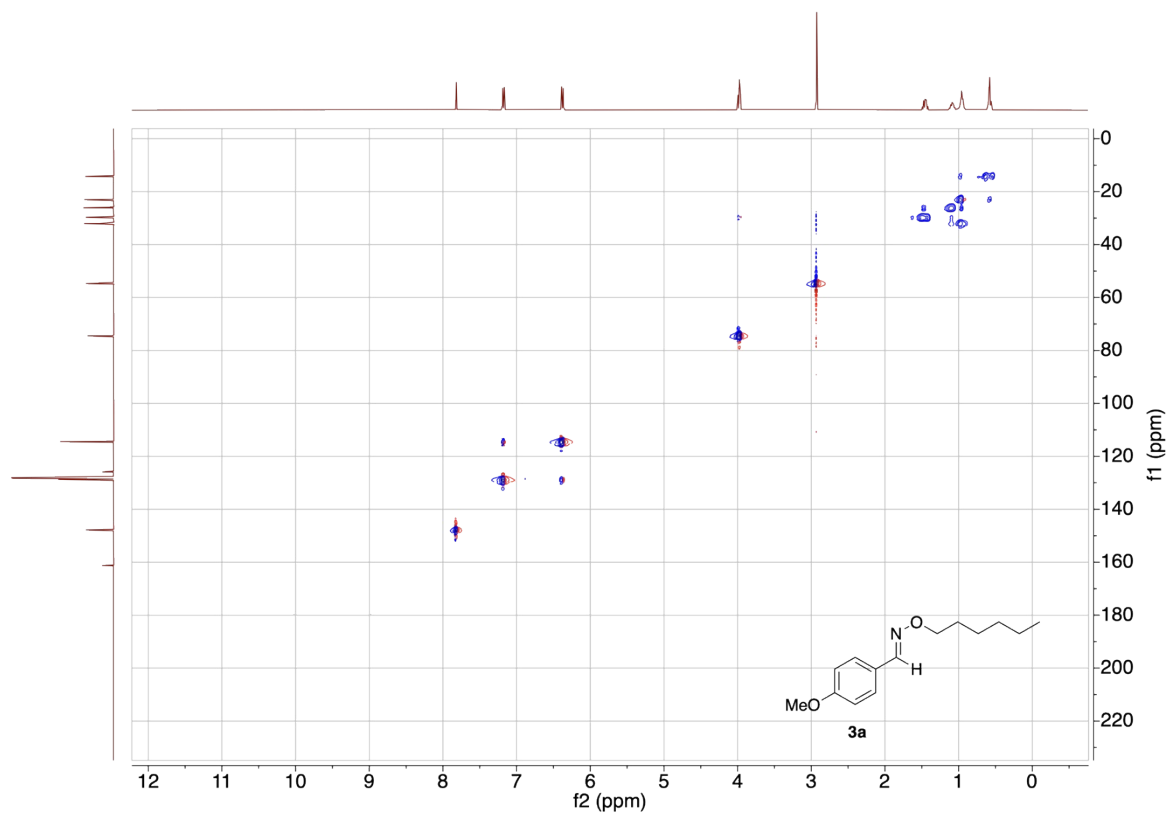


Figure S22. HSQC spectra of compound 3a

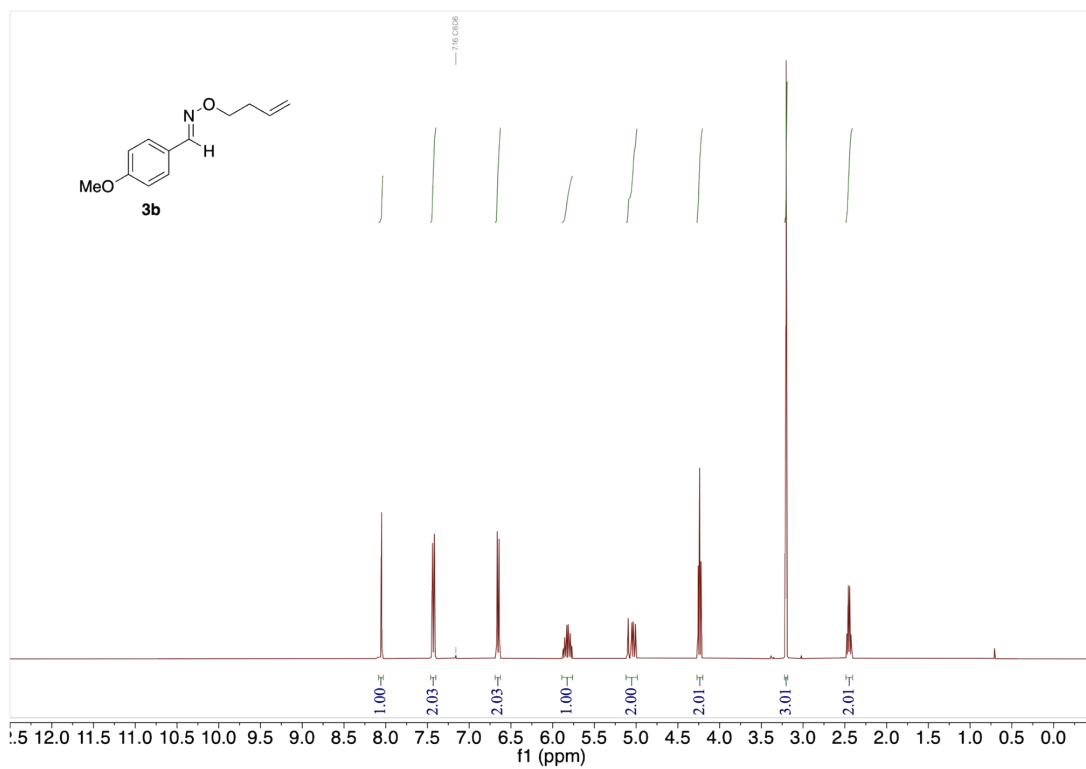
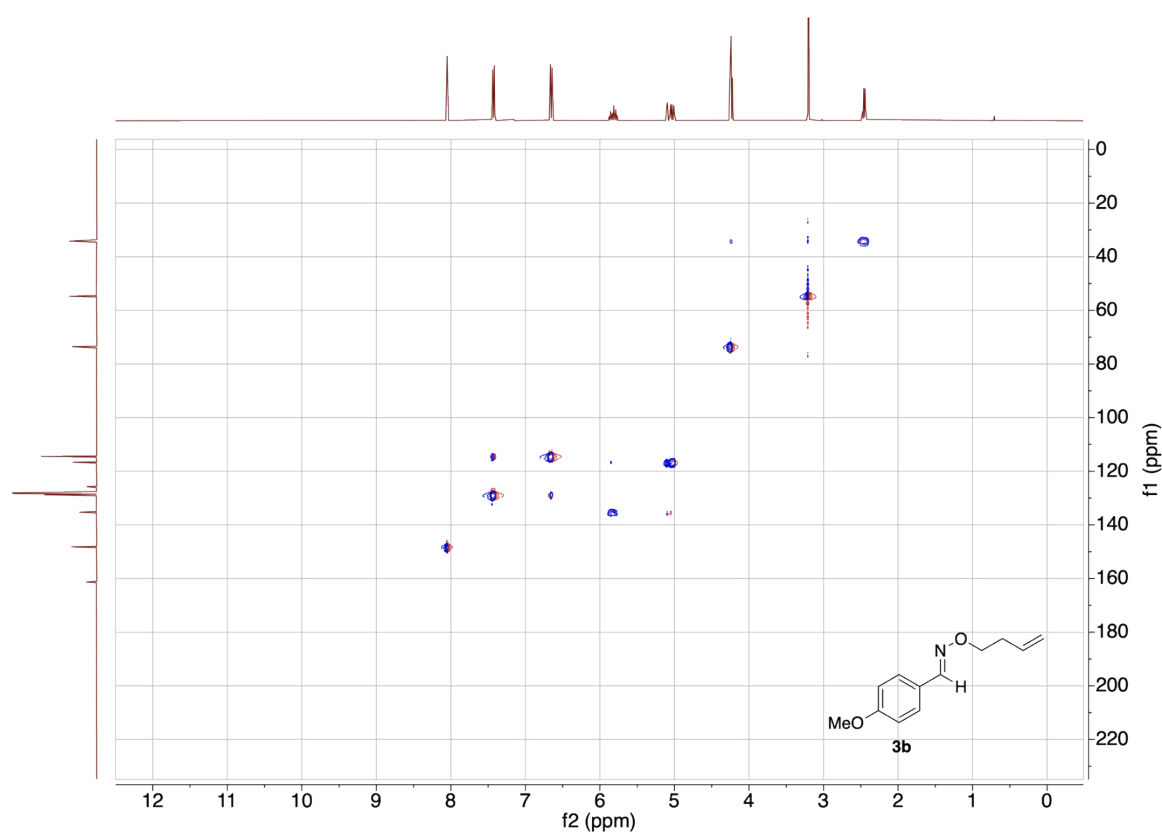
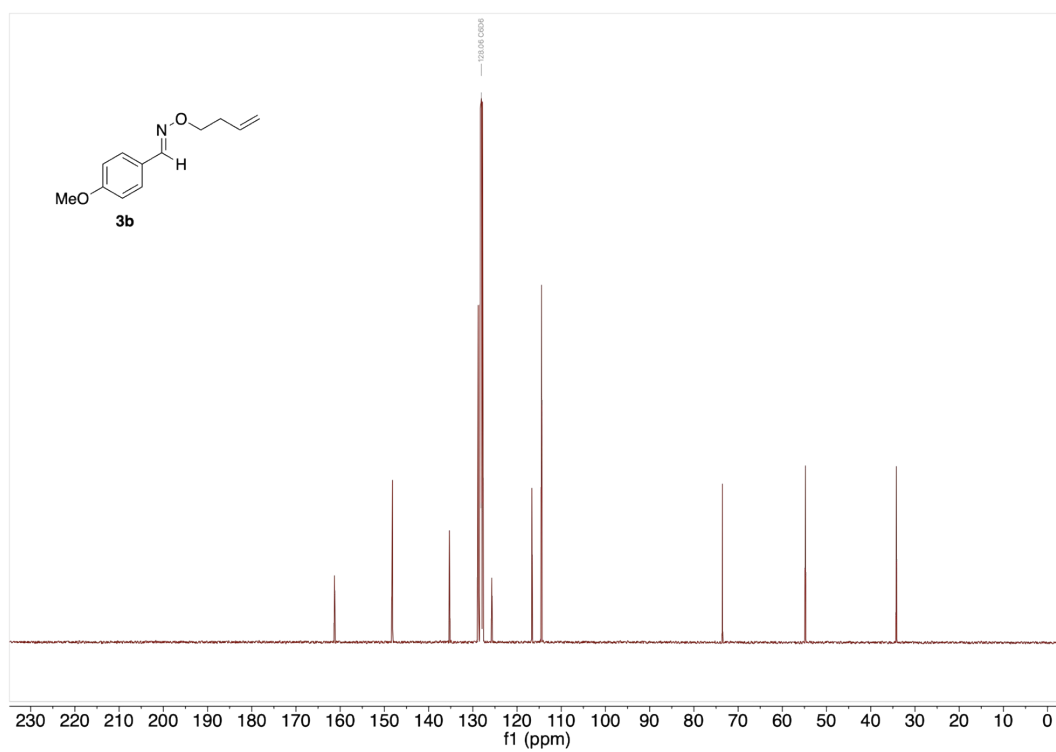
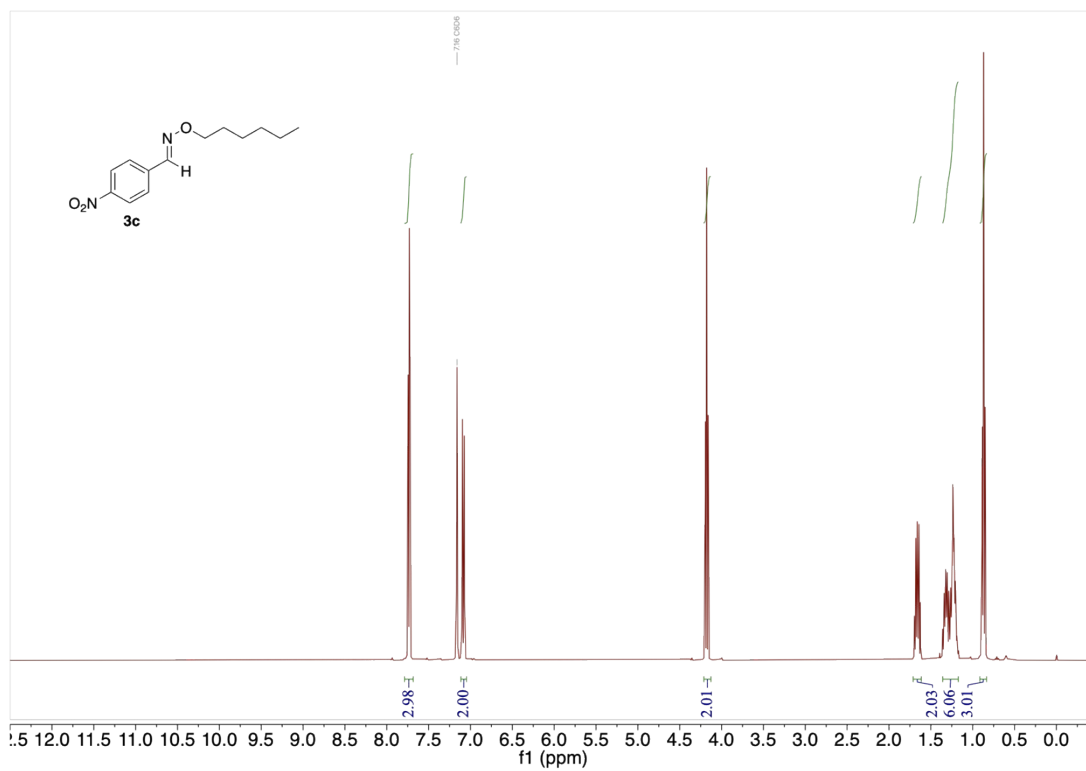
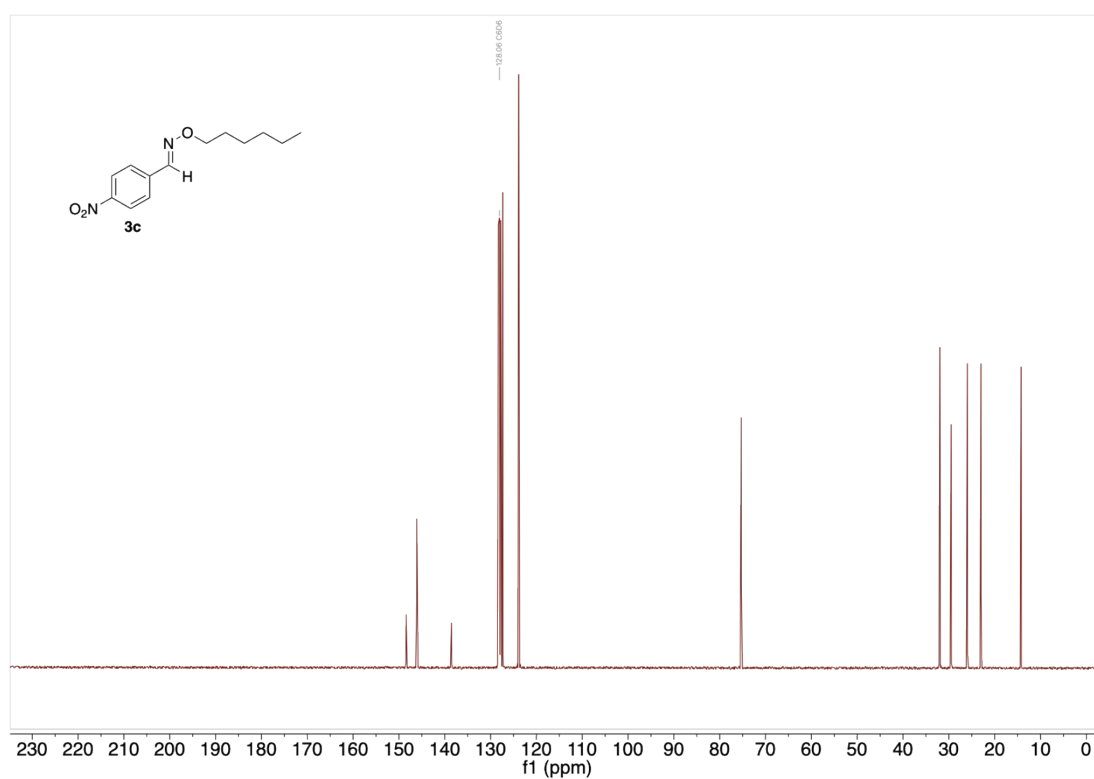


Figure S23. <sup>1</sup>H-NMR spectra of compound 3b





**Figure S26.** <sup>1</sup>H-NMR spectra of compound **3c**



**Figure S27.** <sup>13</sup>C-NMR spectra of compound **3c**

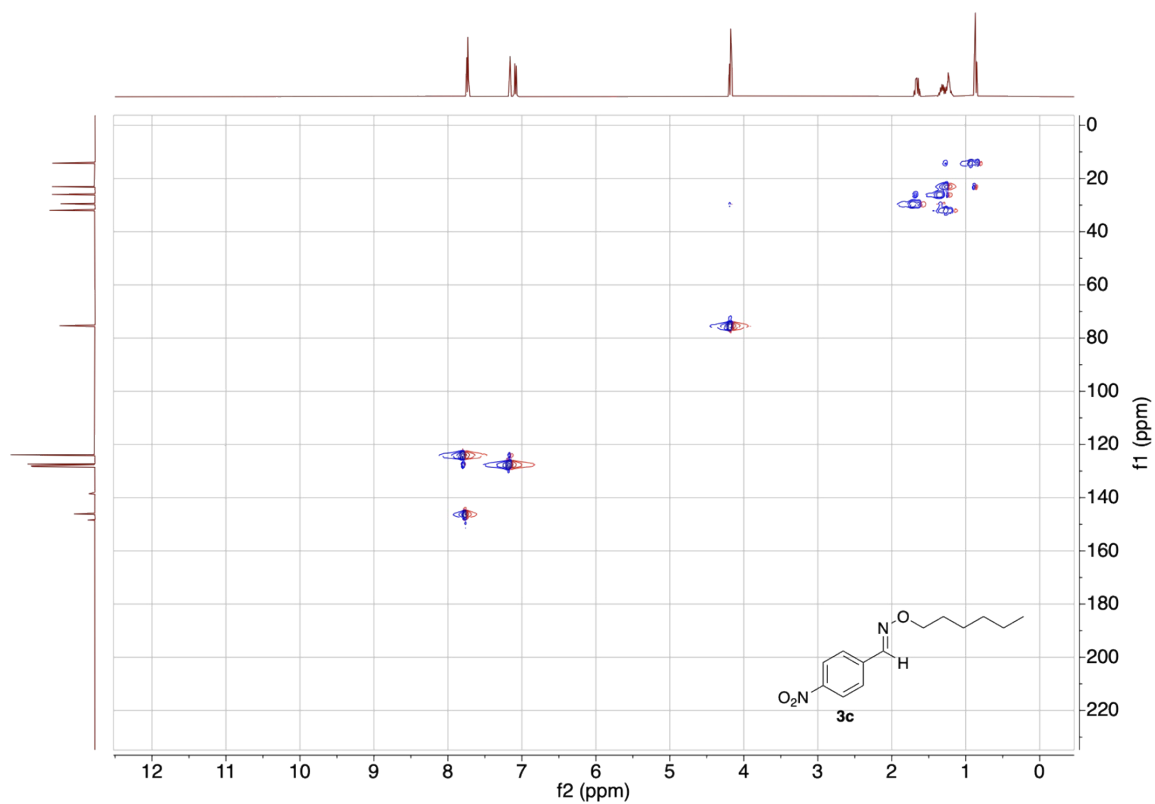


**Figure S28.** HSQC spectra of compound **3c**

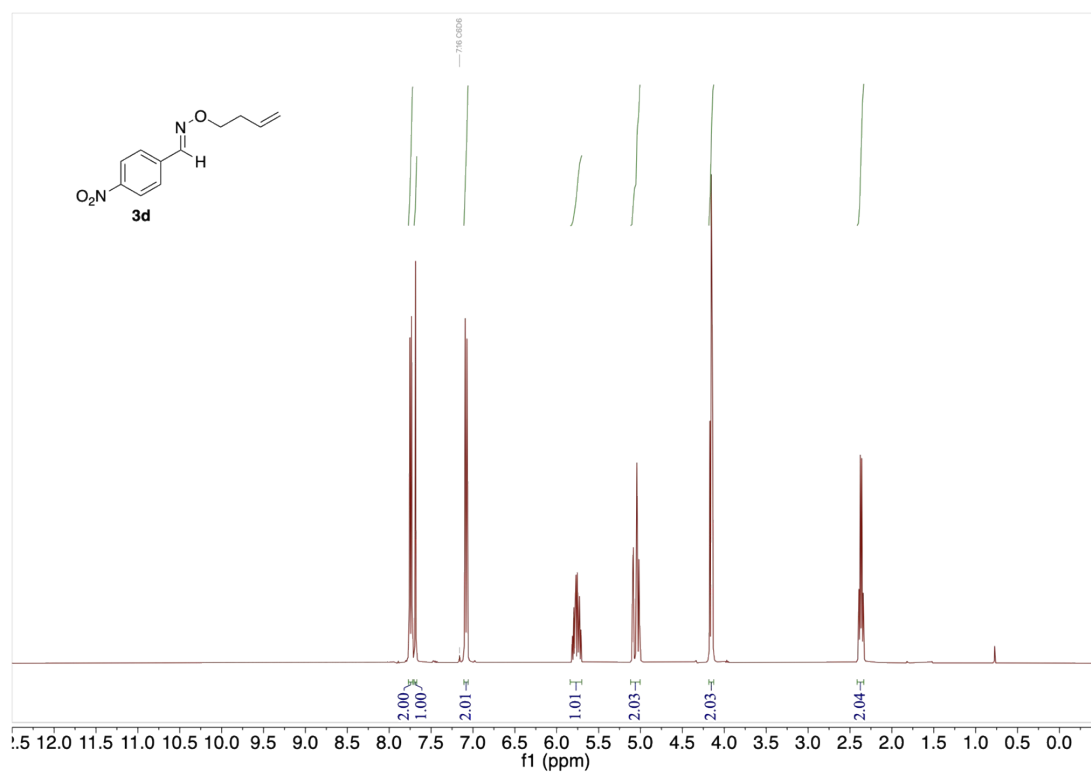


**Figure S29.** <sup>1</sup>H-NMR spectra of compound **3d**

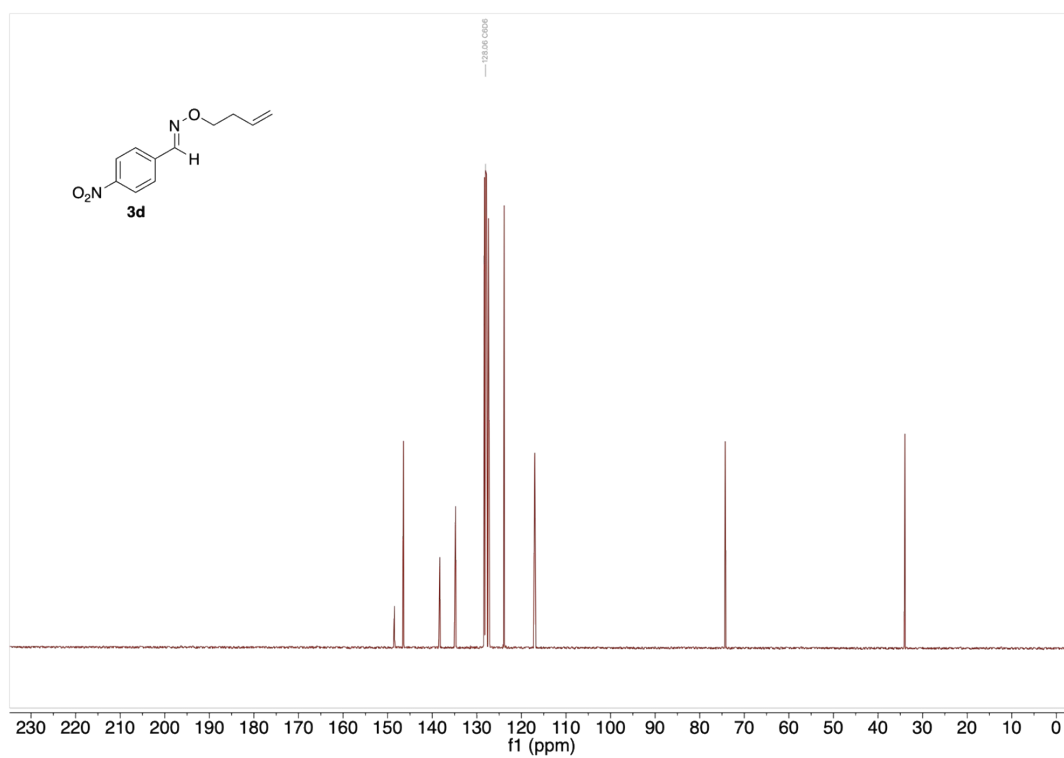


Figure S30. <sup>13</sup>C-NMR spectra of compound 3d

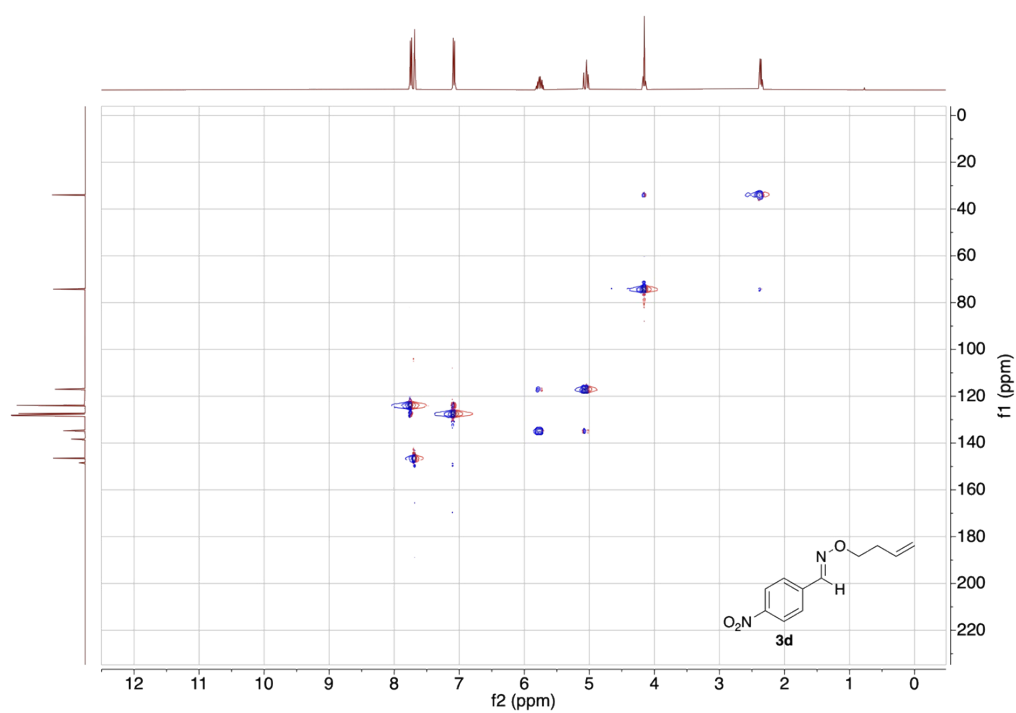
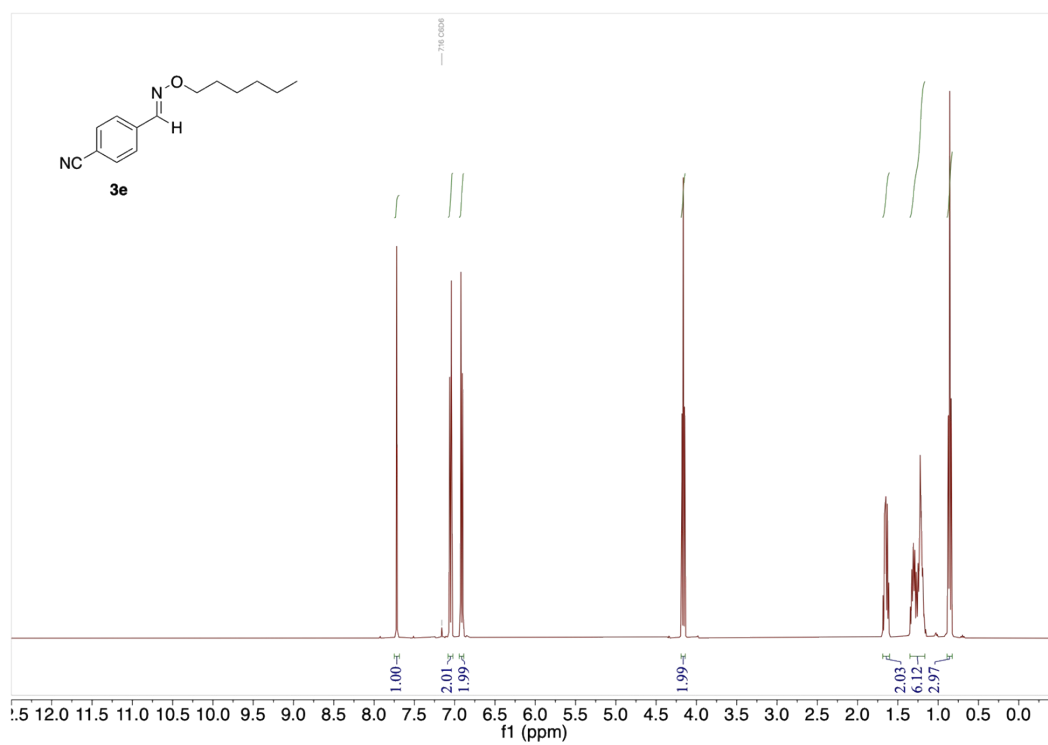
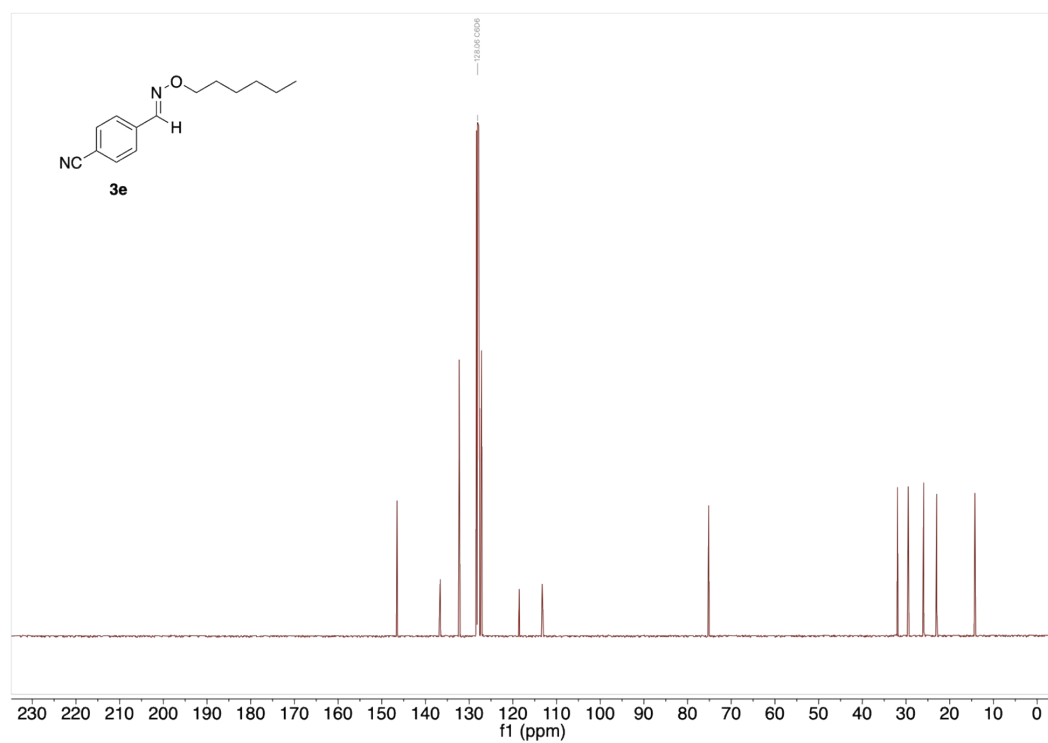


Figure S31. HSQC spectra of compound 3d



**Figure S32.** <sup>1</sup>H-NMR spectra of compound **3e**



**Figure S33.** <sup>13</sup>C-NMR spectra of compound **3**

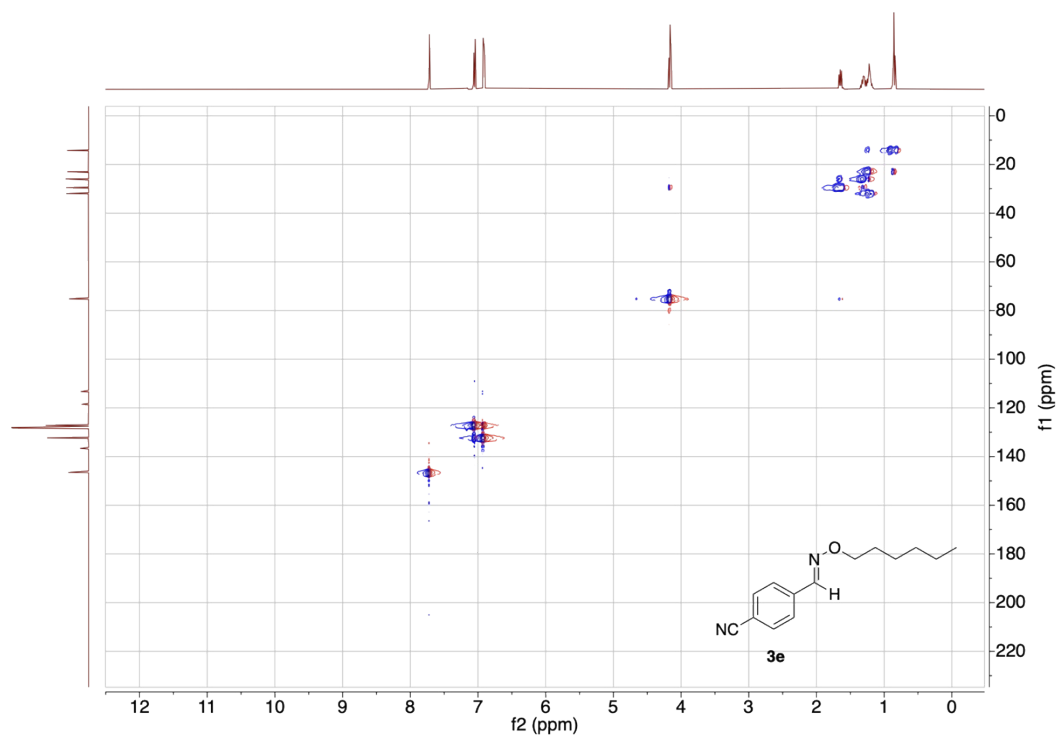


Figure S34. HSQC spectra of compound **3e**

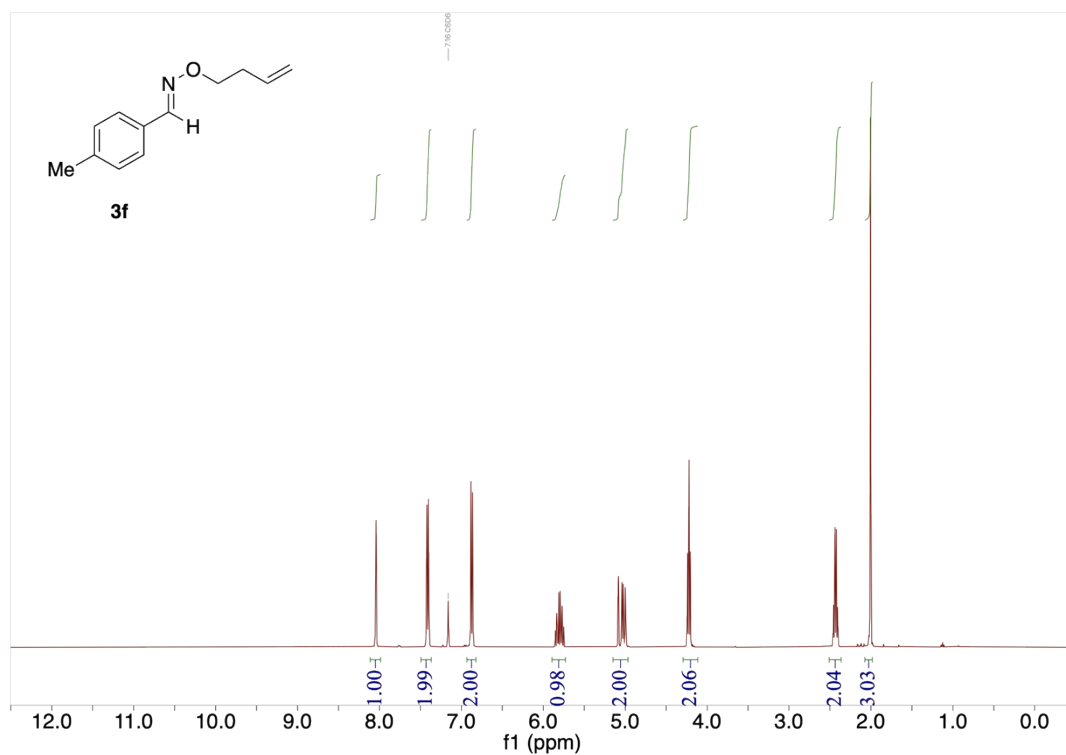


Figure S35. <sup>1</sup>H-NMR spectra of compound **3f**

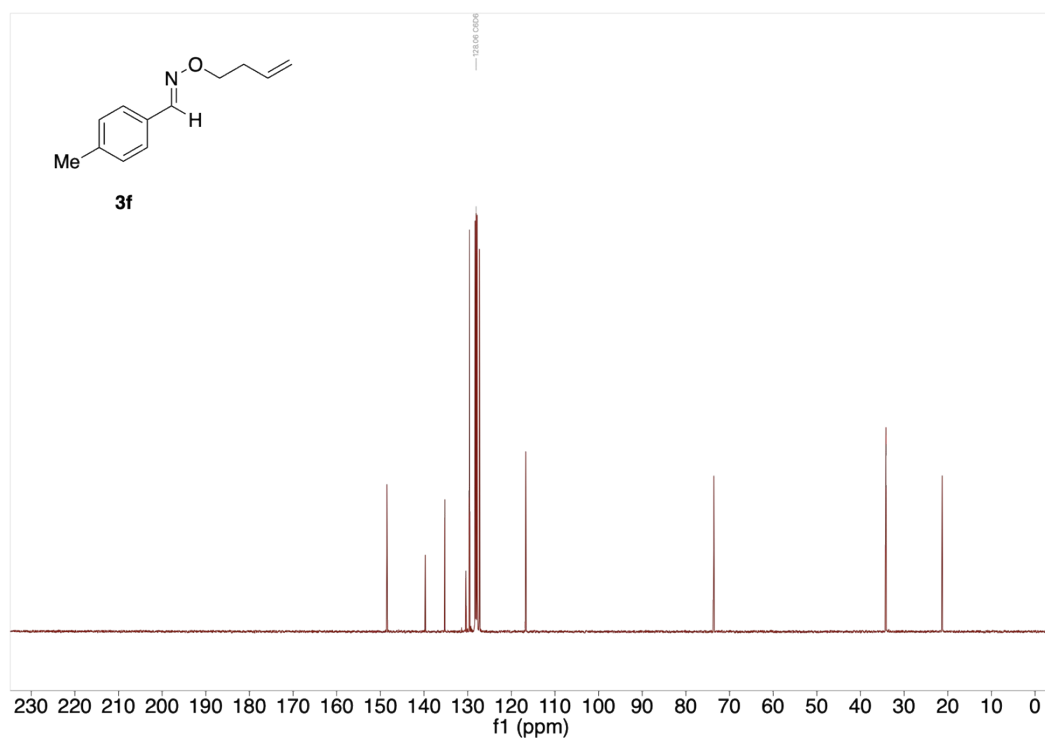


Figure S36. <sup>13</sup>C-NMR spectra of compound 3f

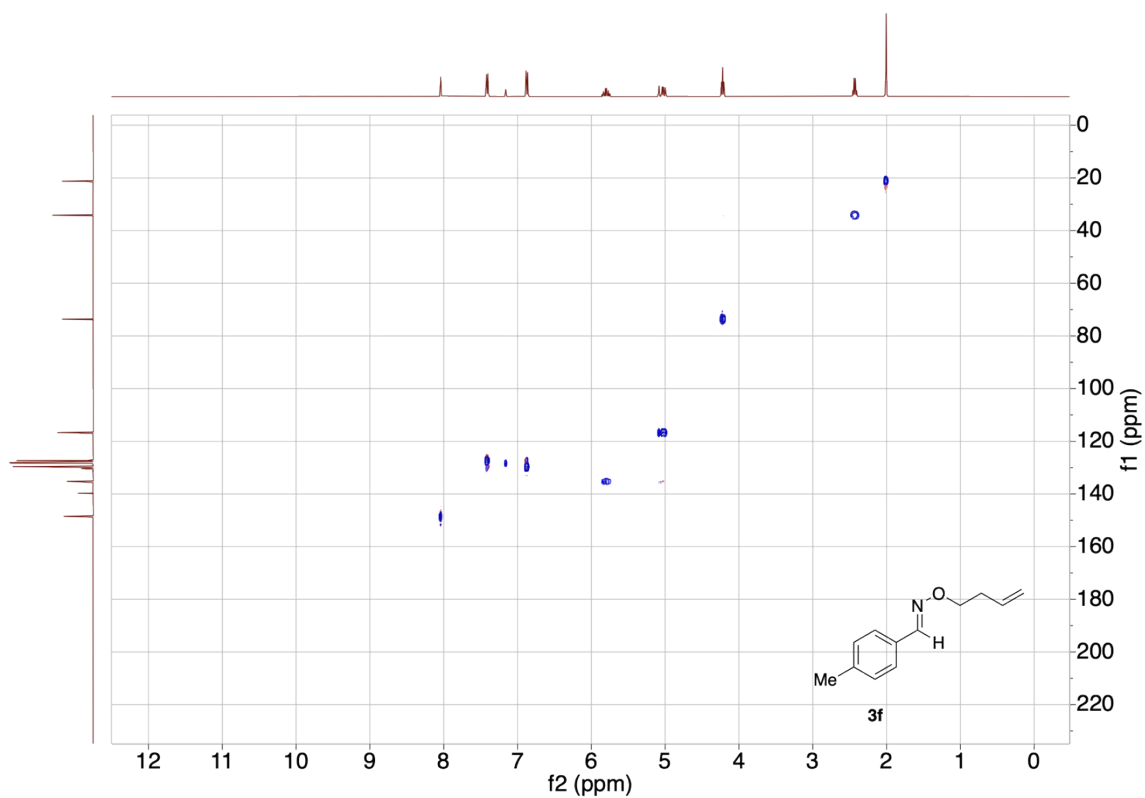


Figure S37. HSQC spectra of compound 3f

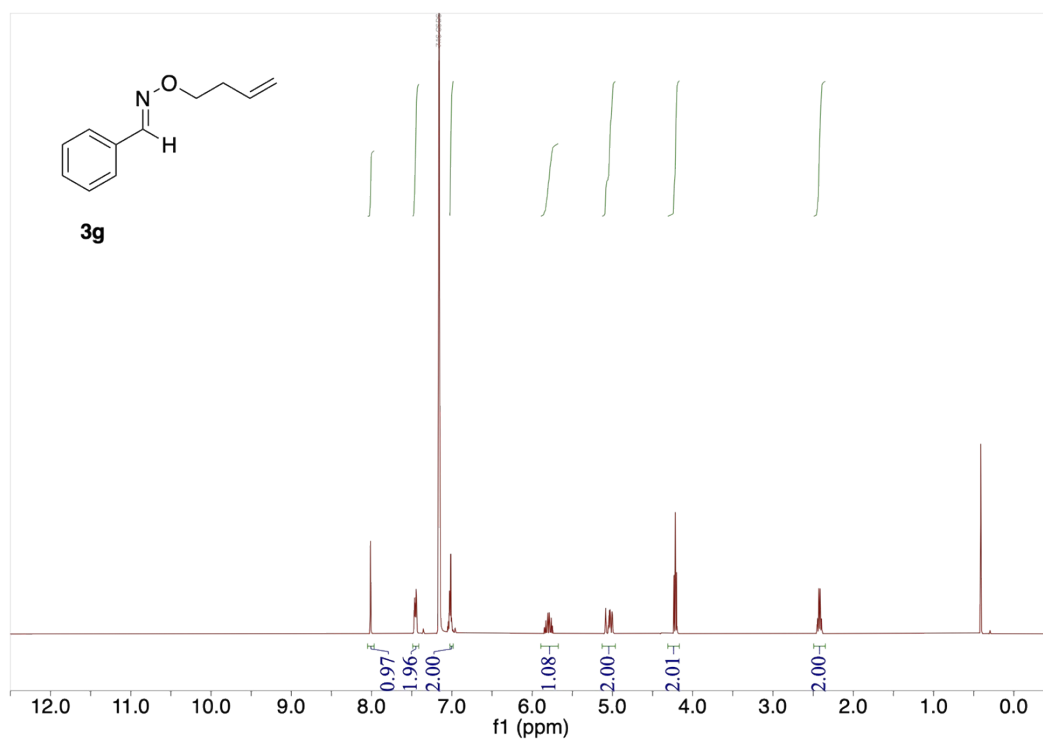


Figure S38. <sup>1</sup>H-NMR spectra of compound 3g

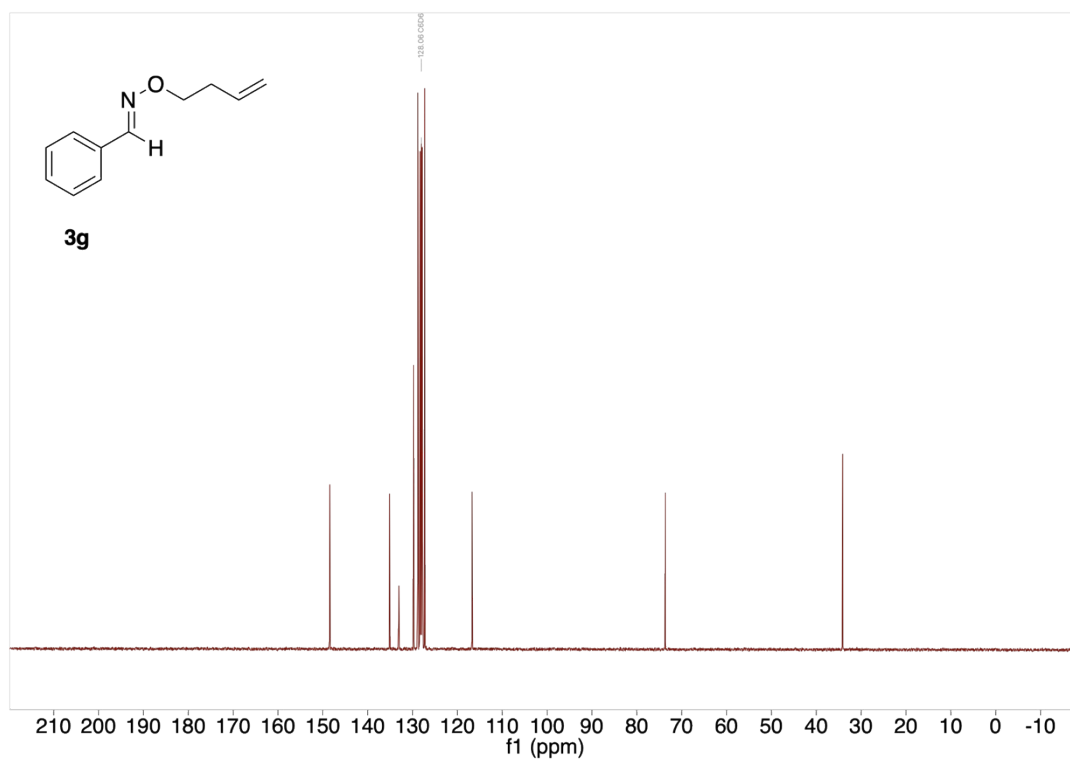


Figure S39. <sup>13</sup>C-NMR spectra of compound 3g

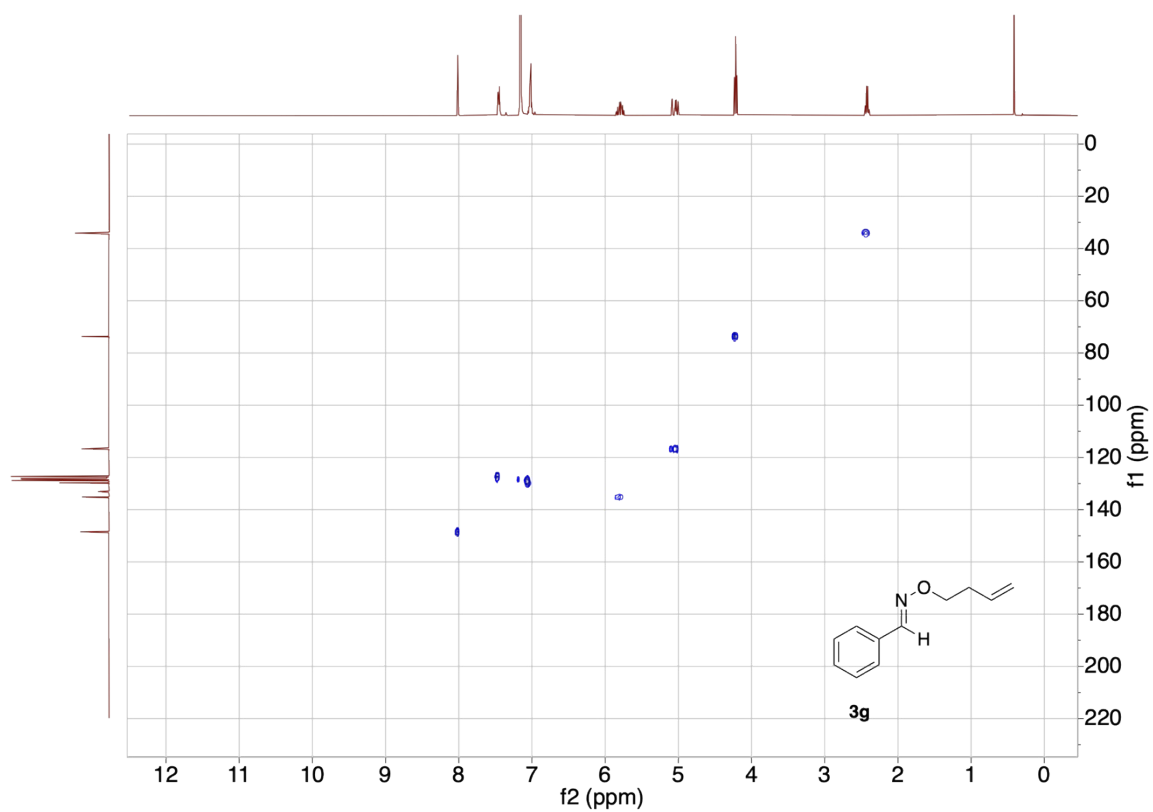


Figure S40. HSQC spectra of compound 3g

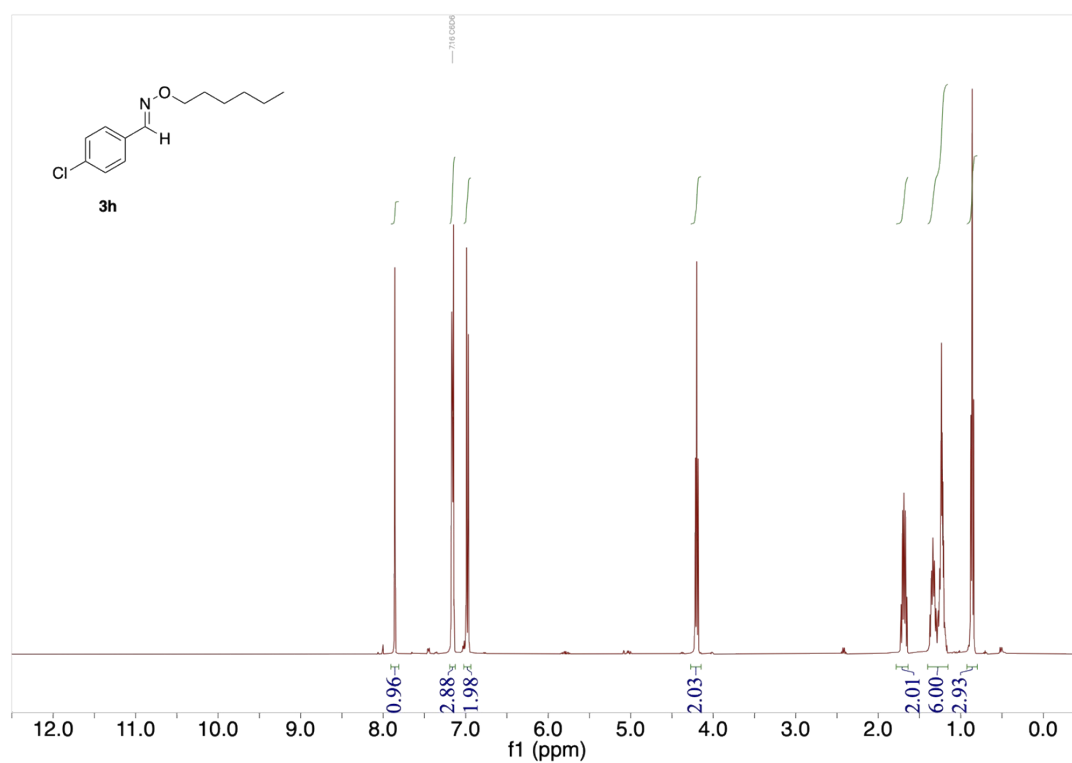


Figure S41. <sup>1</sup>H-NMR spectra of compound 3h

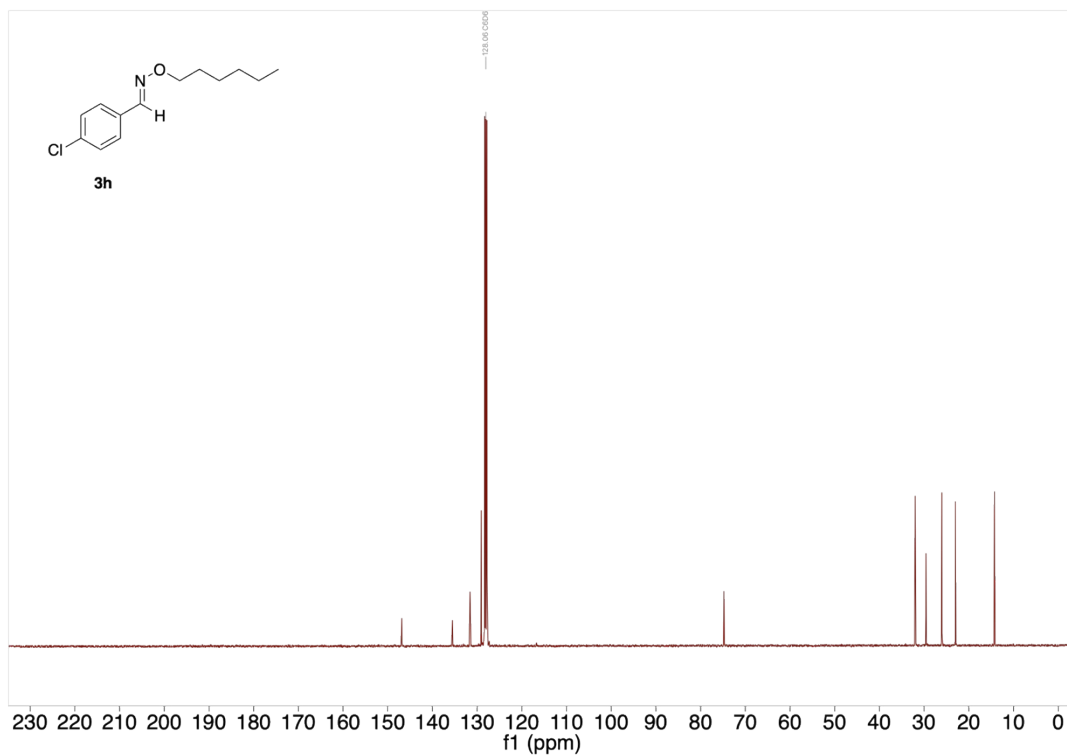


Figure S42.  $^{13}\text{C}$ -NMR spectra of compound **3h**

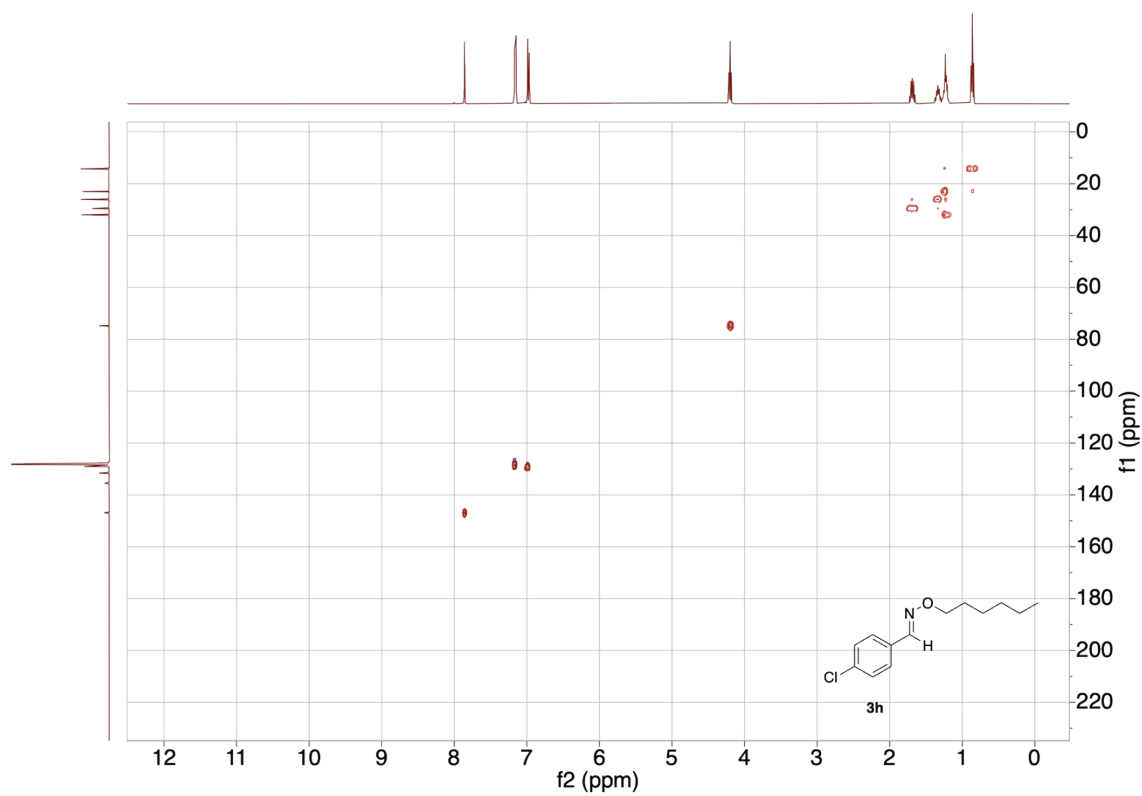


Figure S43. HSQC spectra of compound **3h**

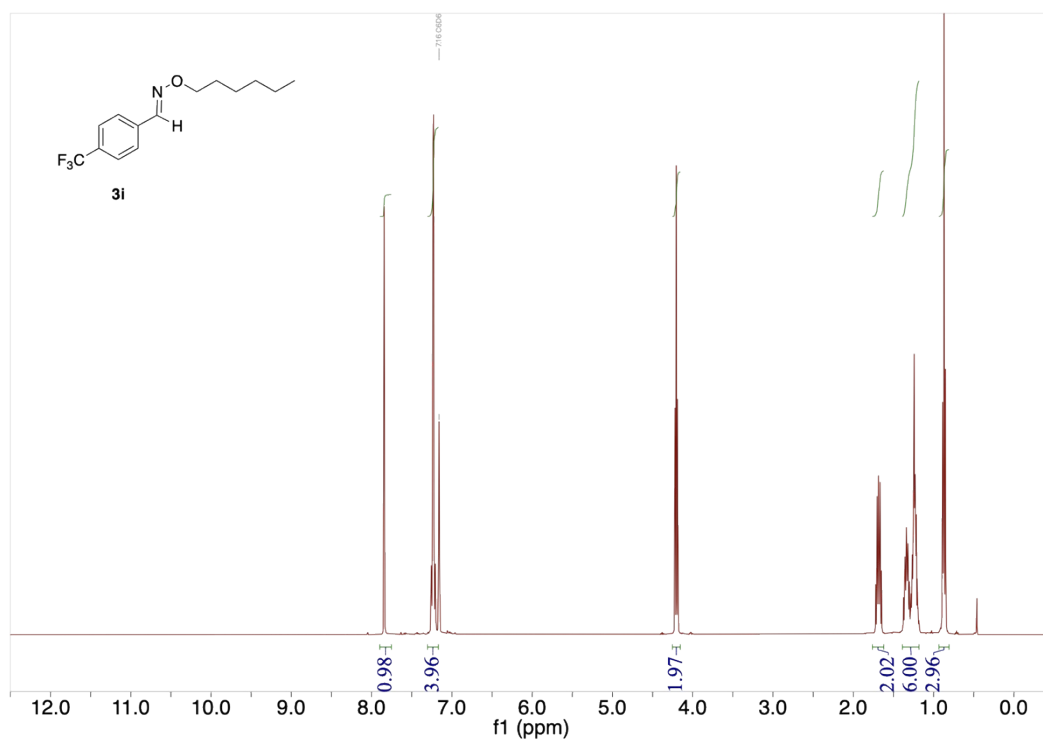


Figure S44. <sup>1</sup>H-NMR spectra of compound **3i**

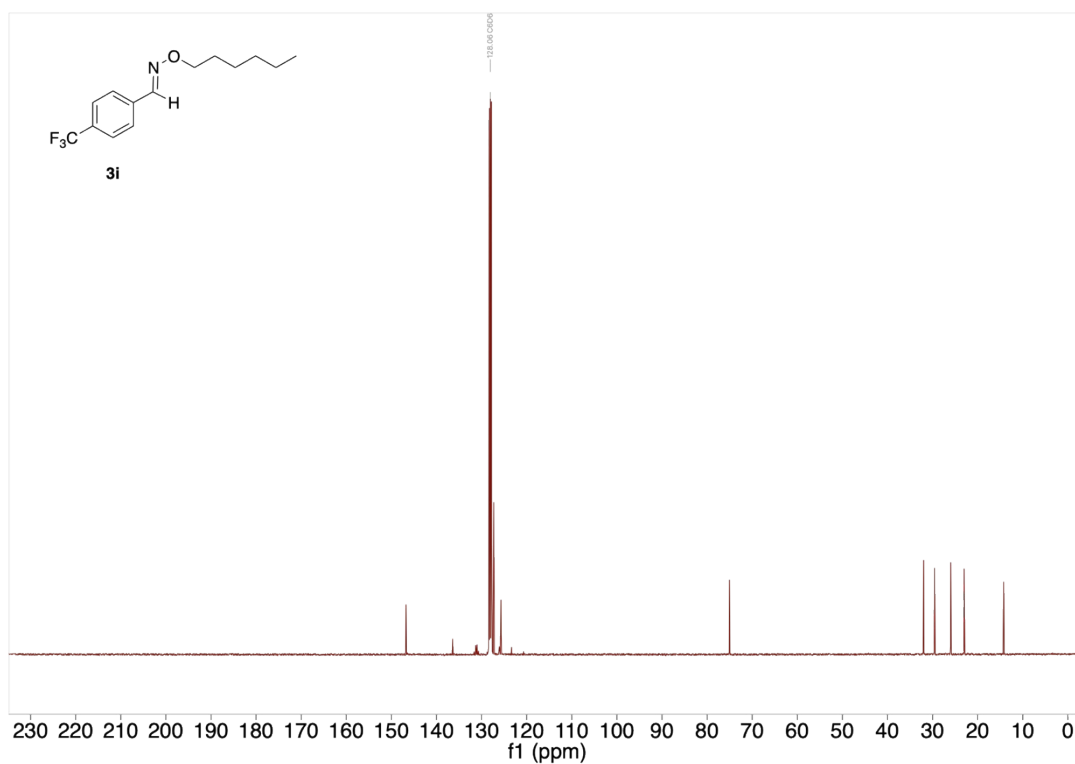


Figure S45. <sup>13</sup>C-NMR spectra of compound **3i**

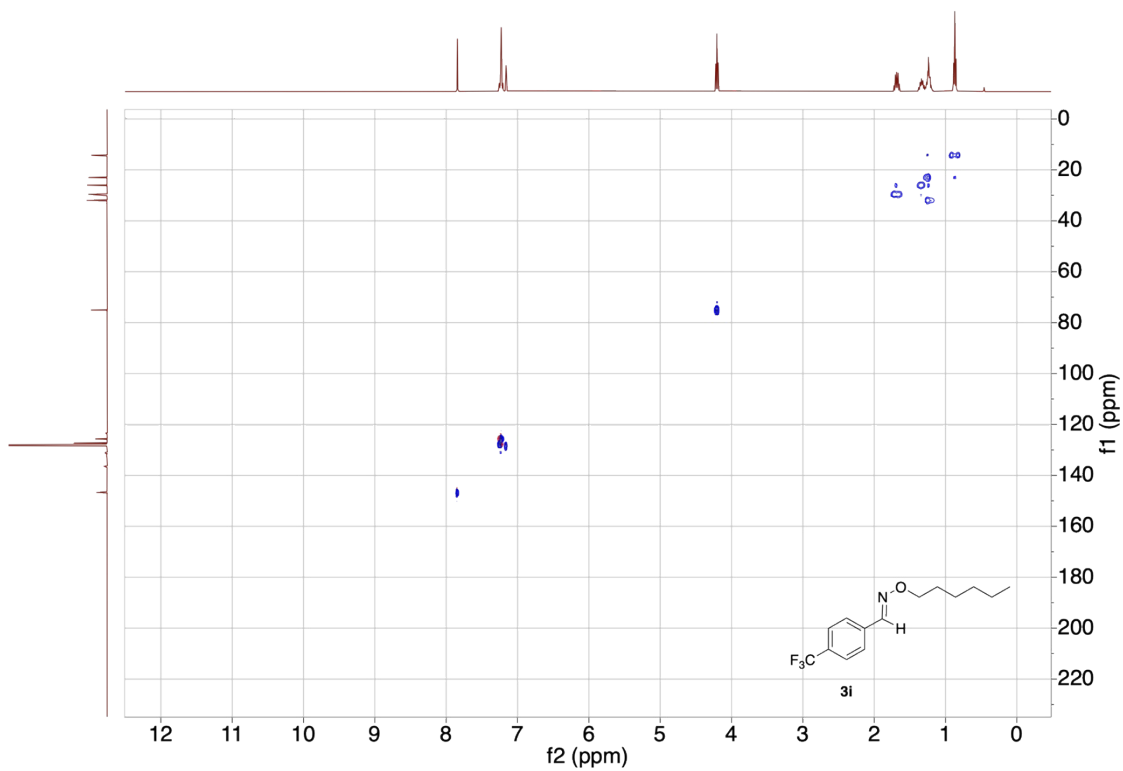


Figure S46. HSQC spectra of compound **3i**

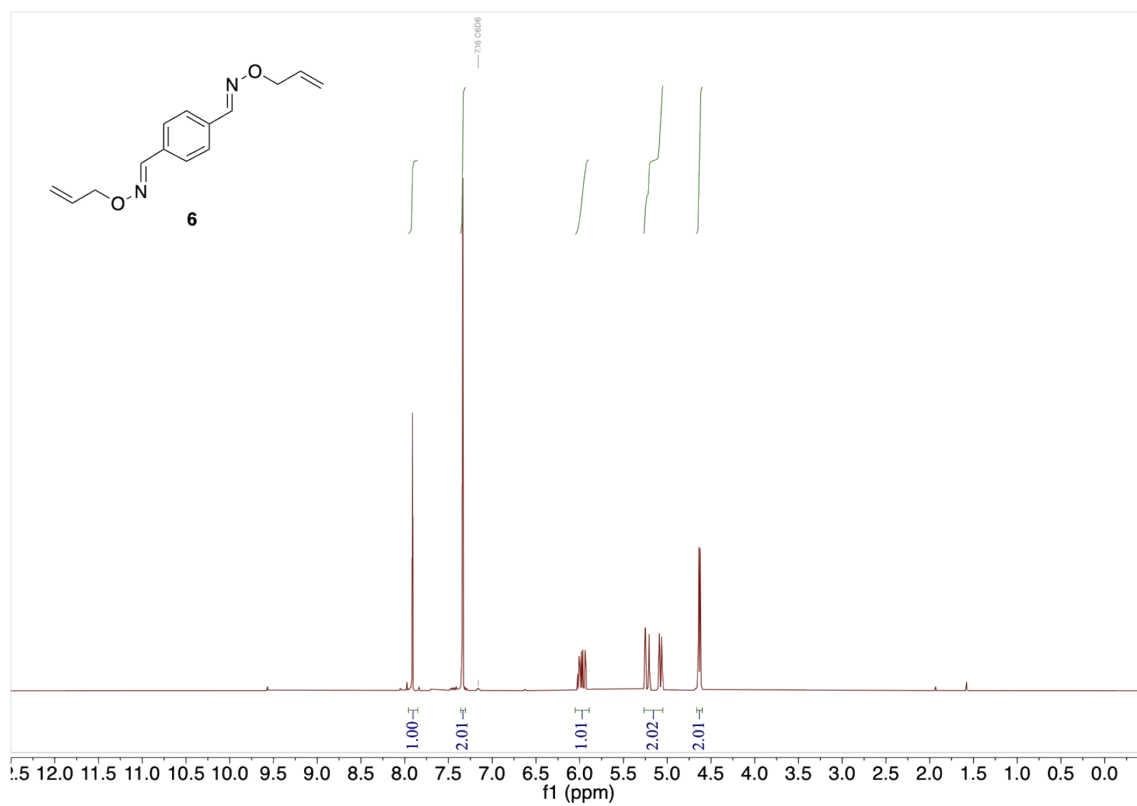
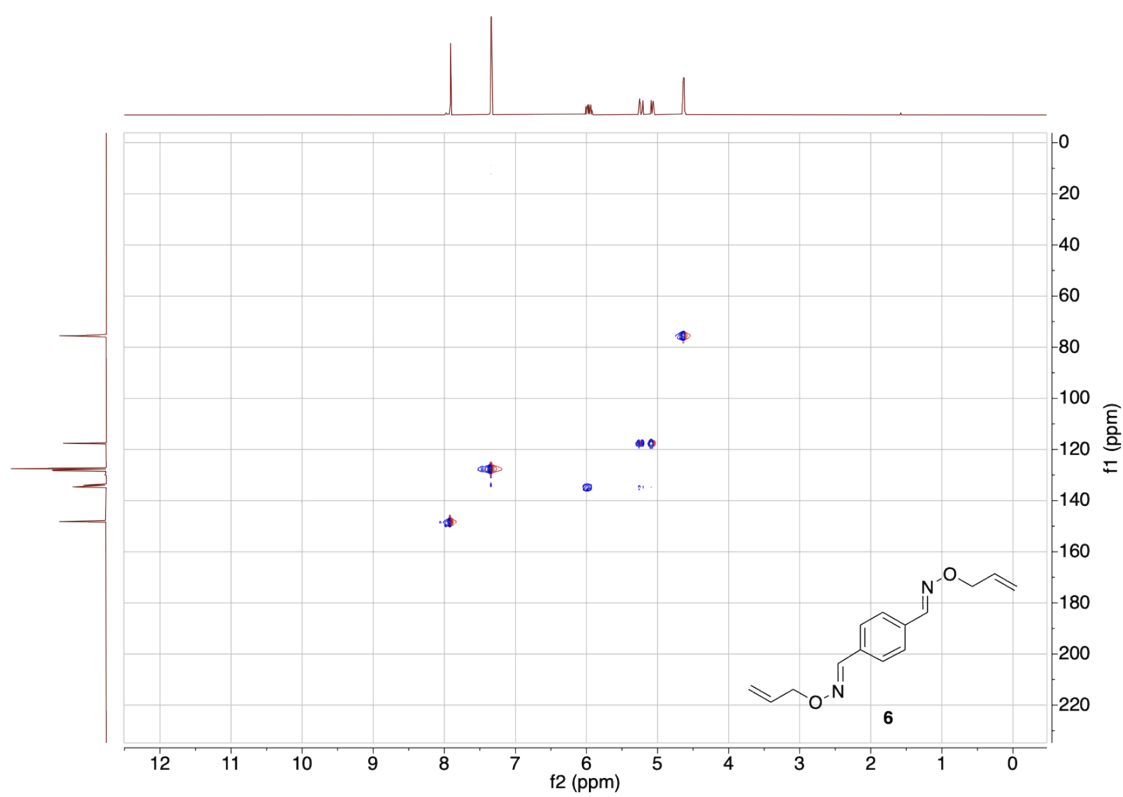
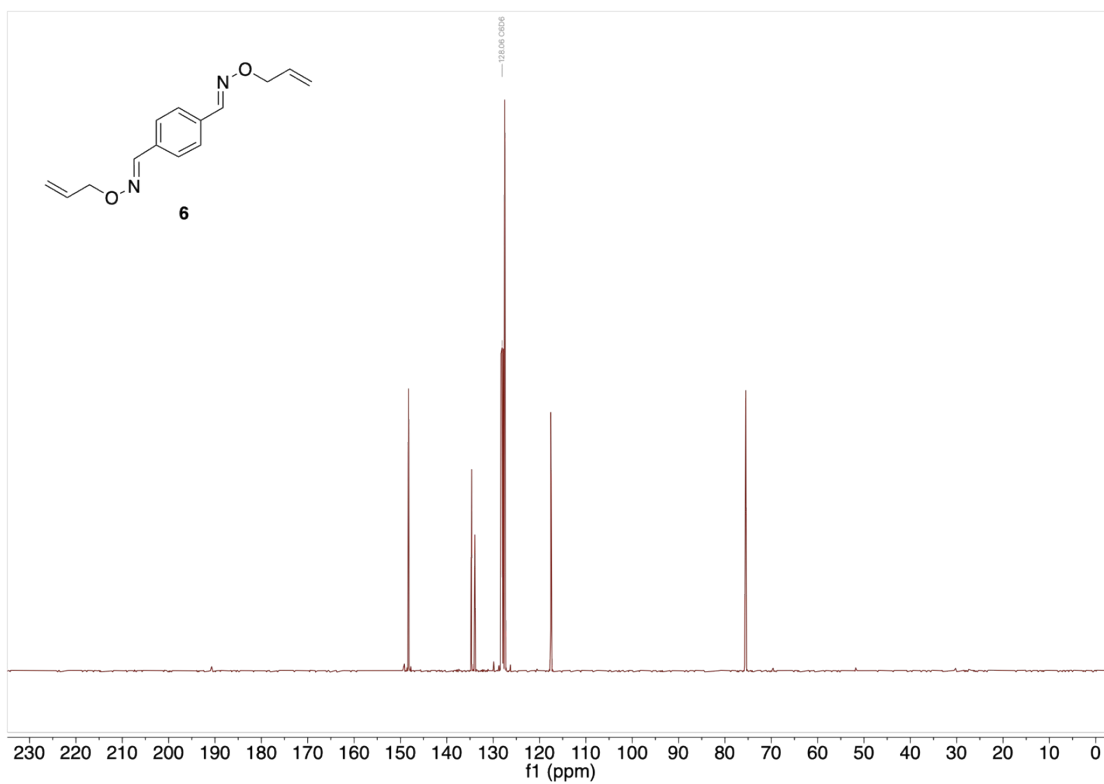
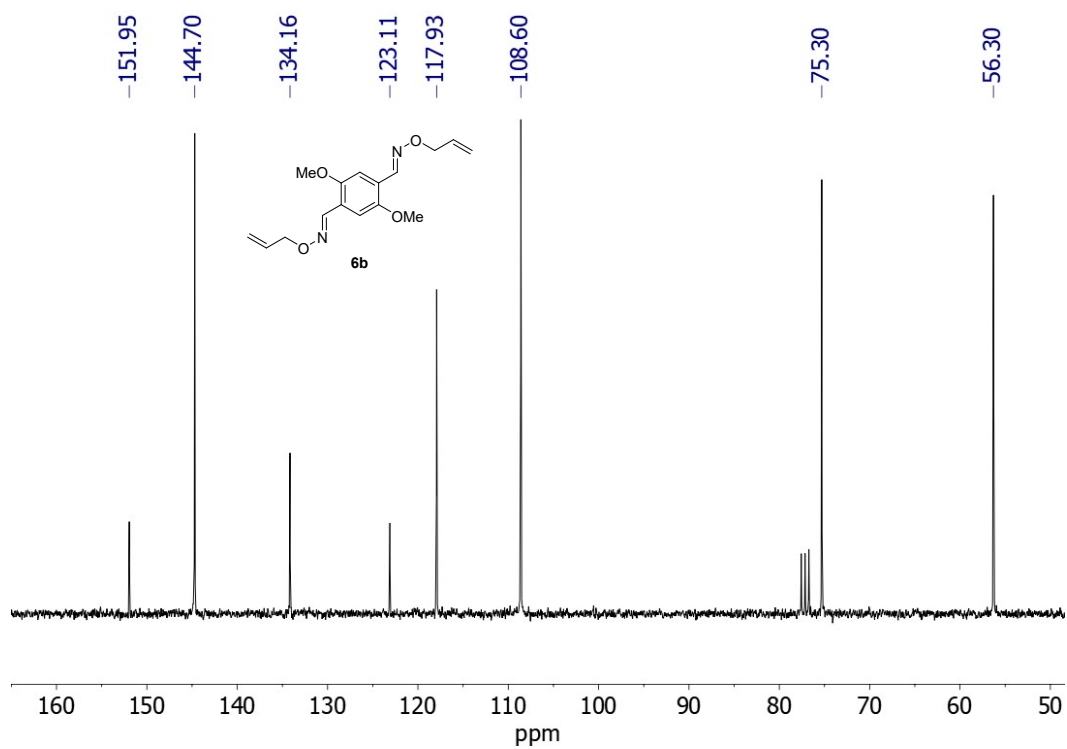
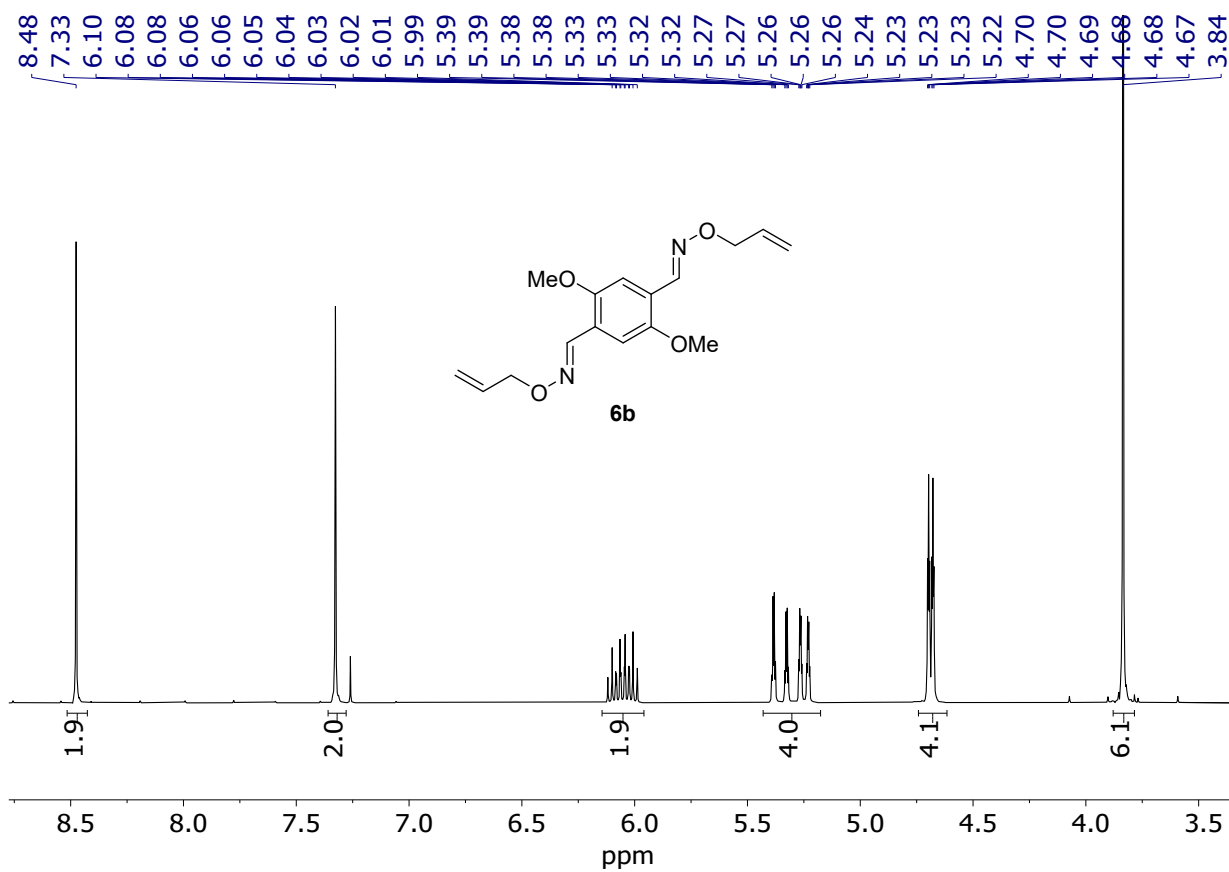


Figure S47.  $^1\text{H}$ -NMR spectra of compound **6a**





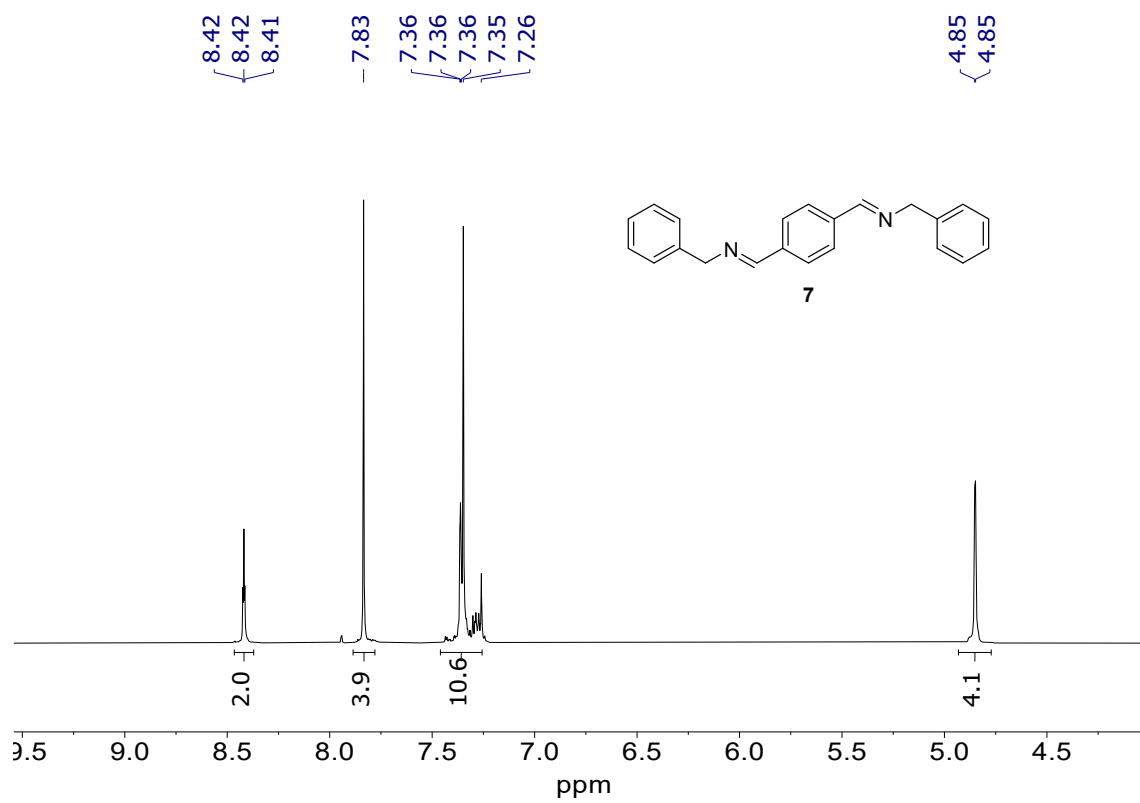
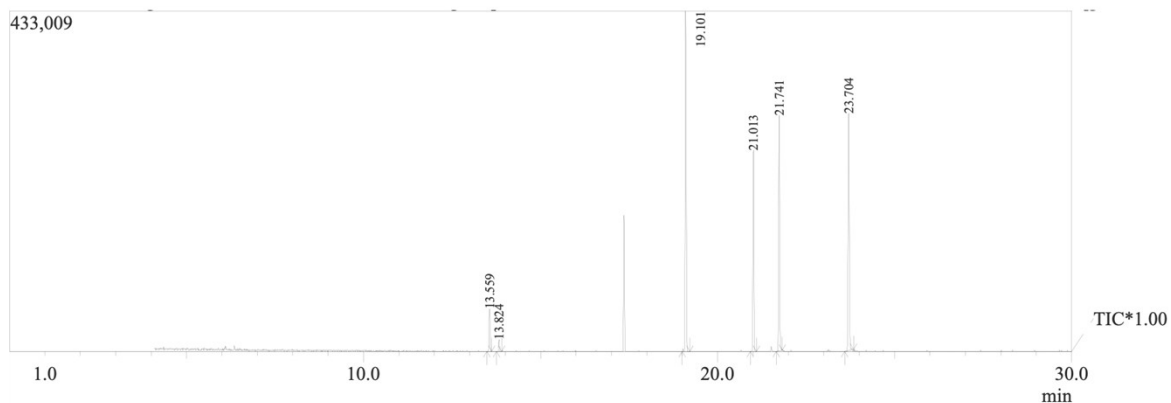


Figure S52. <sup>1</sup>H-NMR spectra of compound 7

# GC-MS CHROMATOGRAM AND MASS SPECTRA

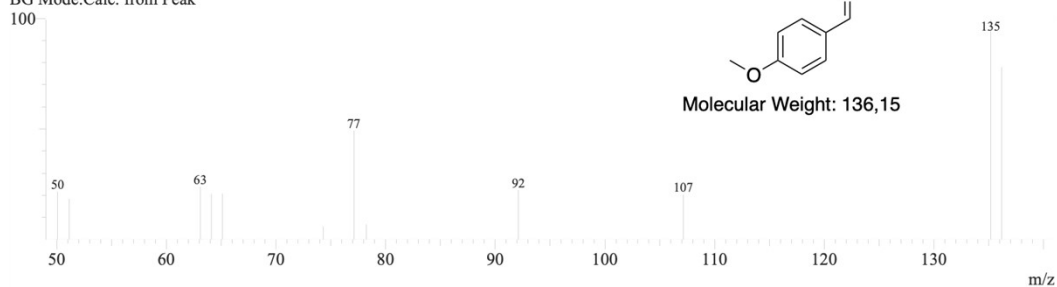


Peak Report TIC

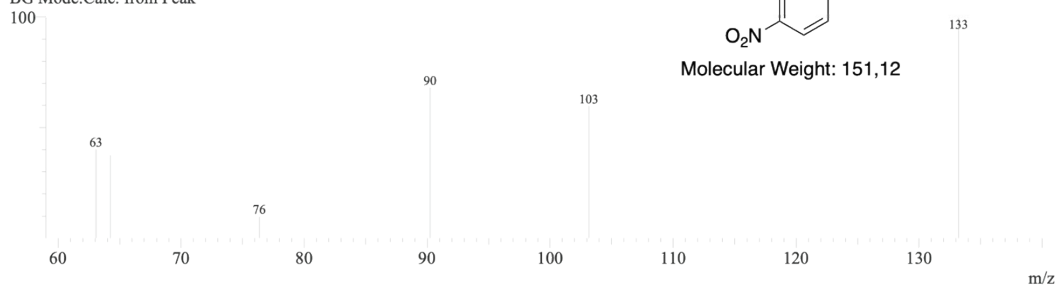
Peak#	R.Time	Area	Area%	Height	Height%	Name
1	13.559	96777	3.59	54088	3.98	
2	13.824	23841	0.88	15217	1.12	
3	19.101	779910	28.90	433009	31.84	
4	21.013	499937	18.52	256036	18.83	
5	21.741	563803	20.89	299750	22.04	
6	23.704	734732	27.22	301682	22.19	
		2699000	100.00	1359782	100.00	

## Spectrum

Peak#:1 R.Time:13.6(Scan#:1136)  
 MassPeaks:12  
 RawMode:Averaged 13.6-13.6(1135-1137)  
 BG Mode:Calc. from Peak



Peak#:2 R.Time:13.8(Scan#:1168)  
 MassPeaks:6  
 RawMode:Averaged 13.8-13.8(1167-1169)  
 BG Mode:Calc. from Peak



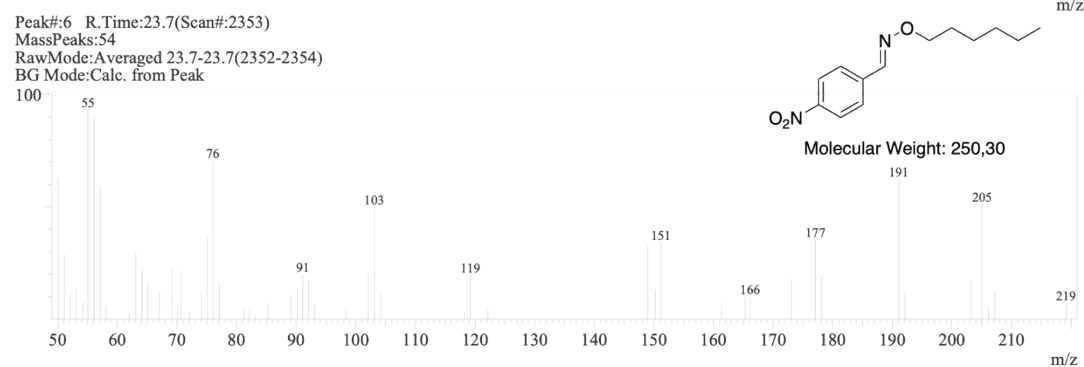
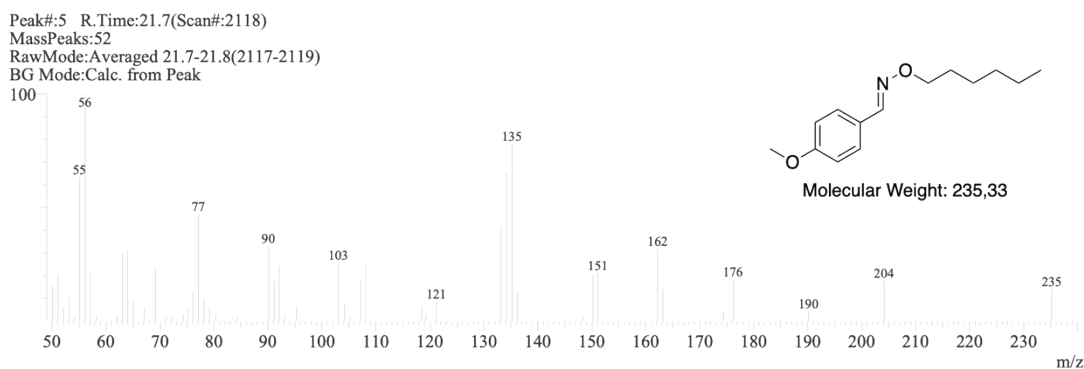
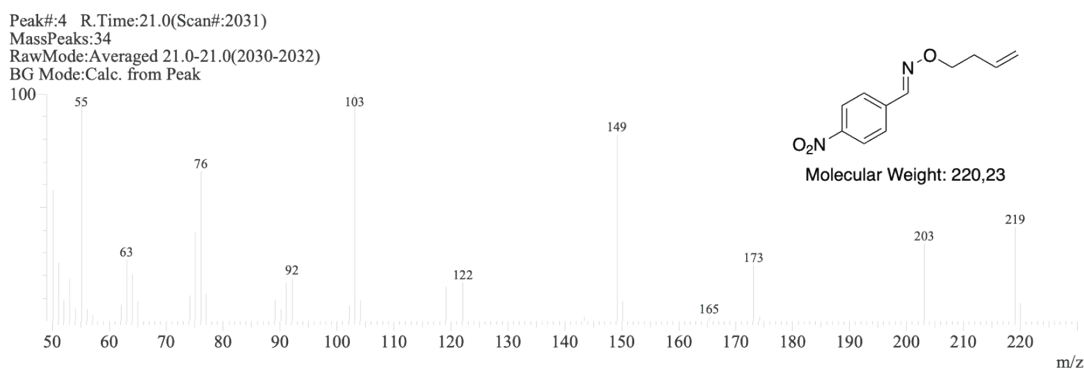
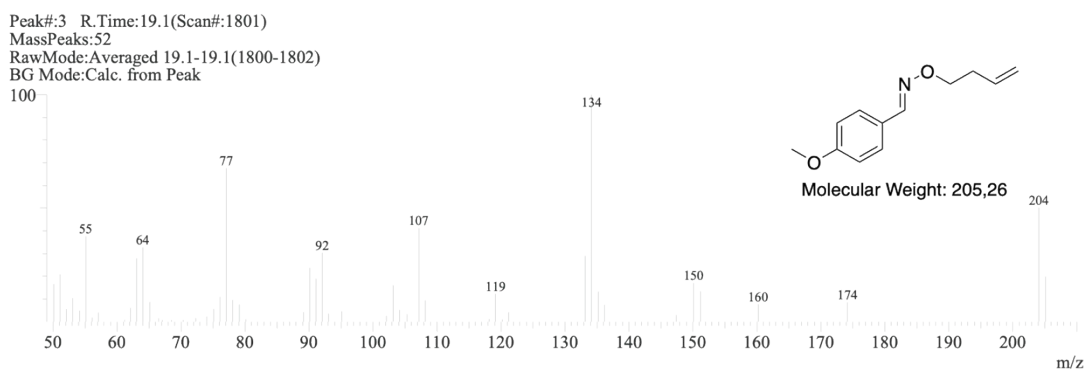


**Figure S53.** GC-MS chromatogram of the crude of the model reaction for oxime metathesis performed between **3b** and **3c** after 120 minutes and the MS spectra relative to the respective peaks.

## REFERENCES

- 1) Ramón, R. S.; Bosson, J.; Diez-González, S.; Marion, N.; Nolen, S. P. Au/Ag-Cocatalyzed Aldoximes to Amides Rearrangement under Solvent- and Acid-Free Conditions. *J. Org. Chem.* **2010**, *75* (4), 1197-1202. DOI: 10.1021/jo902461a
- 2) Koca, M.; Servi, S.; Kirilmis, C.; Ahmedzade, M.; Kazaz, C.; Özbek, B.; Öyuk, G. Synthesis and Antimicrobial Activity of Some Novel Derivatives of Benzofuran: Part 1. Synthesis and Antimicrobial Activity of (benzofuran-2-yl)(3-phenyl-3-methylcyclobutyl) Ketoxime Derivatives. *Eur. J. Med. Chem.* **2005**, *40* (12), 1351-1358. DOI: 10.1016/j.ejmech.2005.07.004
- 3) Llorente, O.; Agirre, A.; Calvo, I.; Olaso, M.; Tomovska, R.; Sardon, H. Exploring the Advantages of Oxygen-Tolerant Tiole-ene Polymerization Over Conventional Acrylare Free Radical Photopolymerization Processes for Pressure-Sensitive Adhesive. *Polym. J.* **2021**, *53*, 1195-1204. DOI: 10.1038/s41428-021-00520-z
- 4) Neese, F.; Wennmo, F.; Becker, U.; Riplinger, C. The ORCA Quantum Chemistry Program Package. *J. Chem. Phys.* **2020**, *152* (22), 224108. <https://doi.org/10.1063/5.0004608>.
- 5) Pracht, P.; Bohle, F.; Grimme, S. Automated Exploration of the Low-Energy Chemical Space with Fast Quantum Chemical Methods. *Phys. Chem. Chem. Phys.* **2020**, *22* (14), 7169–7192. <https://doi.org/10.1039/C9CP06869D>.
- 6) Bannwarth, C.; Ehlert, S.; Grimme, S. GFN2-XTB—An Accurate and Broadly Parametrized Self-Consistent Tight-Binding Quantum Chemical Method with Multipole Electrostatics and Density-Dependent Dispersion Contributions. *J. Chem. Theory Comput.* **2019**, *15* (3), 1652–1671. <https://doi.org/10.1021/acs.jctc.8b01176>.
- 7) Caldeweyher, E.; Bannwarth, C.; Grimme, S. Extension of the D3 Dispersion Coefficient Model. *J. Chem. Phys.* **2017**, *147* (3), 034112. <https://doi.org/10.1063/1.4993215>.
- 8) Spicher, S.; Grimme, S. Robust Atomistic Modeling of Materials, Organometallic, and Biochemical Systems. *Angew. Chem. Int. Ed.* **2020**, *59* (36), 15665–15673. <https://doi.org/10.1002/anie.202004239>.
- 9) Grimme, S.; Brandenburg, J. G.; Bannwarth, C.; Hansen, A. Consistent Structures and Interactions by Density Functional Theory with Small Atomic Orbital Basis Sets. *J. Chem. Phys.* **2015**, *143* (5), 054107. <https://doi.org/10.1063/1.4927476>.
- 10) Grimme, S.; Ehrlich, S.; Goerigk, L. Effect of the Damping Function in Dispersion Corrected Density Functional Theory. *J. Comput. Chem.* **2011**, *32* (7), 1456–1465. <https://doi.org/10.1002/jcc.21759>.
- 11) Grimme, S.; Hansen, A.; Ehlert, S.; Mewes, J.-M. R 2 SCAN-3c: A “Swiss Army Knife” Composite Electronic-Structure Method. *J. Chem. Phys.* **2021**, *154* (6), 064103. <https://doi.org/10.1063/5.0040021>.
- 12) Ásgeirsson, V.; Arnaldsson, A.; Jónsson, H. Efficient Evaluation of Atom Tunneling Combined with Electronic Structure Calculations. *J. Chem. Phys.* **2018**, *148* (10), 102334. <https://doi.org/10.1063/1.5007180>.